

Understanding Novel Superconductors with *ab-initio* Calculations

Lilia Boeri

Abstract This chapter gives an overview of the progress in the field of computational superconductivity. Following the MgB₂ discovery (2001), there has been an impressive acceleration in the development of methods based on Density Functional Theory to compute the critical temperature and other physical properties of actual superconductors from first-principles. State-of-the-art *ab-initio* methods have reached predictive accuracy for conventional (phonon-mediated) superconductors, and substantial progress is being made also for unconventional superconductors. The aim of this chapter is to give an overview of the existing computational methods for superconductivity, and present selected examples of material discoveries that exemplify the main advancements.

1 Introduction

The aim of this chapter is to offer an up-to-date perspective on the field of *ab-initio* superconductivity and of the related development of numerical methods to compute critical temperatures and other physical properties of superconductors.

The material-specific aspect is what distinguishes *ab-initio* (= from first principles) approaches, based on Density Functional Theory (DFT) and its extensions, from other theoretical approaches to superconductivity, which mainly focus on the general description of the phenomenon. The typical questions addressed by computational superconductivity are: (i) what makes a certain compound a good (or bad) superconductor? (ii) How are its properties modified by external parameters, such as doping, pressure, strain? (iii) Is it possible to find new materials with improved superconducting properties compared to existing ones?

Lilia Boeri
Dipartimento di Fisica, Sapienza Università di Roma, P.le Aldo Moro 2, 00185 Roma, Italy, e-mail:
lilia.boeri@uniroma1.it

The most relevant parameter that defines the performance of a superconductor for large-scale applications is its critical temperature (T_c): this means that addressing the questions above requires the development of methods accurate enough to predict the T_c of a superconductor, and its dependence on external parameters. The progress in this direction, in the last twenty years, has been impressive.

For a large class of superconductors, i.e. conventional, phonon-mediated ones, *ab-initio* methods are now so accurate that the focus of the field is gradually shifting from the description of existing superconductors to the design of new materials. The first successful example was the prediction of high- T_c conventional superconductivity in SH_3 (2014). [1, 2]

For unconventional superconductors, which comprise two of the most studied classes of materials, the high- T_c cuprates [3] and Fe-based superconductors, [4] *ab-initio* approaches are still far from being predictive, but it is becoming more and more widely accepted that the single-particle electronic structure determines crucial properties of these materials, such as the symmetry of the superconducting gap and the behavior of magnetic excitations.

The topics and the structure of this chapter have been specifically thought to illustrate the parallel progress in *ab-initio* methods and material research for superconductors. I have chosen three discoveries that I consider the fundamental milestones of this process: (a) The report of superconductivity in MgB_2 in 2001, which has disproved the Cohen-Anderson limit for conventional superconductors; (b) The discovery Fe-based superconductors, which has led to a much deeper understanding of the interplay between electronic structure, magnetism and superconductivity in unconventional superconductors; (c) The discovery of high-temperature superconductivity at Megabar pressures in SH_3 , which has given a spectacular demonstration of the predictive power of *ab-initio* calculations.

Although I will give a general introduction to the theory of superconductivity and briefly describe the most recent advancements in *ab-initio* methods, methodological developments are not the main topic of this chapter: I refer the interested reader to excellent reviews in literature for a detailed discussion. [5, 6, 7] For space reasons, I am also forced to leave out some currently very active directions of superconductivity research, such as topological superconductivity, [8] superconductivity in 2D transition metal dichalcogenides, [9] artificial superlattices [10] and other more traditional topics, such as cuprates and other oxides, [11] fullerenes, [12], layered halonitrides, [13], etc.

On the other hand, have included at the end a short perspective describing possible routes to high- T_c superconductivity which exploit novel developments in experimental and *ab-initio* techniques, since I believe that in the next years the combination of the two may lead to the discovery of many new superconductors.

The structure of the chapter is the following: I will start by giving a concise historical review of the most important discoveries in section 2. In section 3 I will then introduce the basic concepts of superconductivity theory, and describe the most recent developments in *ab-initio* methods. The main body of the paper is contained in Section 4, where, using selected material examples, I will try to give an impression of the rapid progress of the field in the understanding of both conventional and un-

conventional superconductors. Finally, in section 5 I will propose possible practical routes to high- T_c superconductivity.

2 A Brief History of Research in Superconductivity

Superconductivity was discovered more than 100 years ago when H.K. Onnes observed that, when cooled below 4 K, mercury exhibits a vanishing resistivity. [14] Perfect diamagnetism, which is the second fingerprint of a superconductor, was discovered by Meissner and Ochsenfeld around 20 years later. [15] While it was immediately clear that superconductors could have an enormous potential for applications, the low critical temperatures represented an insurmountable obstacle to large-scale applications.

In addition to presenting practical problems, superconductivity proved to be a major challenge also for theorists: fully microscopic theories of superconductivity - the Bardeen-Cooper-Schrieffer (BCS) and Migdal-Eliashberg (ME) theories - were developed only after almost fifty years after the original discovery; [16, 17, 18, 19, 20, 21]. They describe superconductivity as due to the condensation of pairs of electrons of opposite spin and momentum (Cooper pairs), held together by an attractive *glue*.¹ In conventional superconductors, the glue is provided by phonons (lattice vibrations), but other excitations such as plasmons, spin fluctuations etc can also mediate the superconducting pairing.

The understanding of the microscopic mechanism of superconductivity did not lead to any immediate, appreciable progress in the search for new superconductors; this translated into a general skepticism towards theory, which is well exemplified by one of the Matthias' rules for superconductivity (*stay away from theorists!*). Indeed, rather than a predictive theory, ME theory was long considered a sophisticated phenomenological framework to describe existing superconductors, while the search for new materials was (unsuccessfully) guided by semi-empirical rules. Even worse, two leading theorists used ME theory to demonstrate the existence of an intrinsic limit of around 25 K to the T_c of *conventional* superconductors. Although conceptually wrong, the *Cohen-Anderson limit* is still cited today as an argument against high- T_c superconductivity. [22]

The notion of an upper limit to T_c was first challenged by the discovery of the first unconventional superconductors, the cuprates, in 1986. [3] In contrast to conventional superconductors, which above T_c behave as ordinary metals, cuprates exhibit a complex phase diagram, with many coexisting phases and physical phenomena (charge and spin density waves, metal-insulator transitions, transport anomalies etc). In 1987 a cuprate, YBCO, broke the liquid N₂ barrier, with a T_c of 92 K, [23] causing a general excitement in the media about a possible *superconducting revolution*; the highest T_c ever attained in this class is 156 K. [24] Despite almost thirty years of research, and many different proposals, a quantitative theory of supercon-

¹ We will treat here only the case of so-called *boson-exchange* superconductors, and not other mechanisms, such as resonant valence bond, hole superconductivity, etc

ductivity in the cuprates is still lacking; furthermore, their large-scale applicability is also limited due to their high brittleness and manufacturing costs. [25]

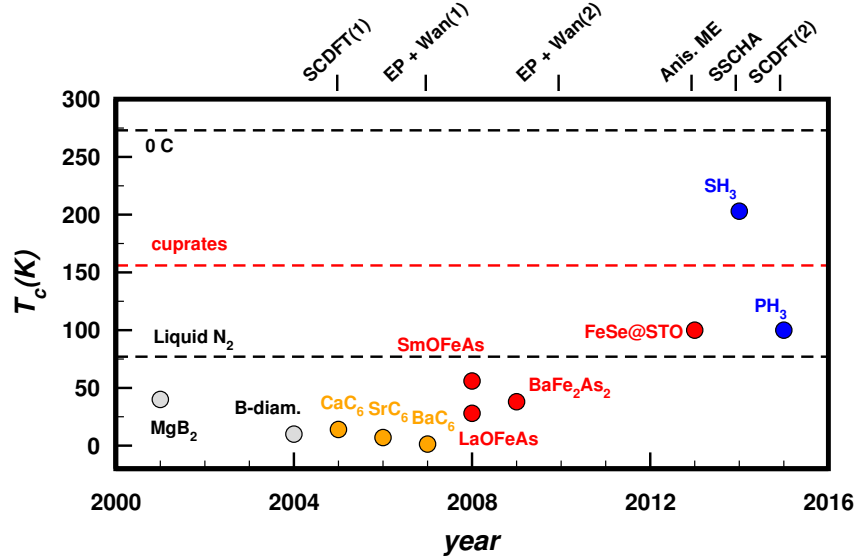


Fig. 1 Main Developments in the field of Superconductivity in the 21st century: The T_c 's of the most important experimental discoveries as a function of year are shown as colored symbols. The top axis reports the most important methodological developments in *ab-initio* superconductivity: Superconducting Density Functional Theory (*SCDF(1)*), [26, 27] electron-phonon interaction with Wannier functions (*EP+WAN(1)* and *EP+WAN(2)*), [5, 28, 29] *ab-initio* anisotropic ME theory (*Anis. ME*), [30, 7] (stochastic) self-consistent harmonic approximation (*SSCHA*), [31] *ab-initio* spin-fluctuations (*SCDF(2)*). [32, 33].

The search for new materials took a different turn at the beginning of this century, when a T_c of 39 K was reported in a simple *s-p* binary compound, magnesium diboride (MgB₂). [34] In contrast to the cuprates, MgB₂ is a conventional superconductor. In less than two years, *ab-initio* calculations provided a key quantitative understanding of very specific aspects of superconductivity in this material, such as two-gap superconductivity, anharmonicity, role of magnetic and non-magnetic impurities, doping, etc. [35, 36, 37, 38, 39, 40] This stimulated a renewed enthusiasm in the search for new superconductors and, in parallel, the development of accurate *ab-initio* methods to model them.

Indeed, in the last seventeen years superconductivity has been discovered in B-doped semiconductors, [41, 42], intercalated graphites, [43] unconventional Fe-based superconductors [4] and, finally, high-pressure hydrides. [1, 44] The T_c 's as a function of the year of their discovery are shown as colored symbols in Fig. 1. The most important methodological developments are reported on the top axis: Superconducting Density Functional Theory [26, 27], electron-phonon interaction with

Wannier functions [28, 29, 5], *ab-initio* anisotropic ME theory [7, 30], (stochastic) self-consistent harmonic approximation, [31], *ab-initio* spin-fluctuations. [32, 33].

Thanks to these advancements, *ab-initio* calculations for conventional superconductors have now reached an accuracy which gives them fully predictive power. Methods are being developed also to treat other types of interactions, such as plasmons and spin fluctuations, [32, 33, 45] and parameter ranges where the standard approximations of strong-coupling ME theory break down. [46]. Combined with the development of efficient methods for *ab-initio* crystal structure prediction and the progress in synthesis and characterization techniques, [47, 48] this opens unprecedented possibilities for material discovery.

3 Methods

In this section I describe the methodological background of computational superconductivity. The first part introduces the main concepts behind the microscopic theories of superconductivity, i.e. the early Bardeen-Cooper-Schrieffer (BCS) theory and the strong coupling Migdal-Eliashberg (ME) theory. Although extremely accurate and elegant, ME theory was for a long time employed only as a semi-phenomenological theory, relying on electronic and vibrational spectra extracted from experiments. Early attempts of obtaining these quantities from Density Functional Theory date back to the early 80's, but with limited success, due to inadequate computational resources and insufficient accuracy of methods to treat phonons and electron-phonon (*ep*) interaction. [49, 50] The required accuracy was only achieved with Density Functional Perturbation Theory (DFPT), [51, 52] and recently substantially increased with Wannier-function interpolation methods. [28, 29, 53]

In a very influential paper, already in 1996, Savrasov and Savrasov demonstrated that linear response calculations combined with Migdal-Eliashberg theory could reproduce the critical temperatures and other properties of elemental metals. [51] However, since at that time the T_c 's of known conventional superconductors were much smaller than those of the cuprates, this result was erroneously perceived as of limited importance.

The report of superconductivity in MgB_2 in 2001 gave a strong impulse to the development of *ab-initio* methods for superconductors, which resulted in two parallel lines of research: *ab-initio* Migdal-Eliashberg theory and Superconducting Density Functional Theory, described in Sect. 3.2. In their fully anisotropic versions, including screened Coulomb interactions, they have a comparable accuracy of 5-10% on the critical temperature, gap, etc. [6, 7, 30] This gives them fully predictive power, and, combined with methods for crystal structure prediction, offers the unprecedented possibility of designing superconductors *ab-initio*, overcoming the practical limitations of experiments.

3.1 A Short Compendium of Superconductivity Theory

The first fully microscopic theory of Superconductivity was formulated by Bardeen, Cooper and Schrieffer in 1957, and is known as BCS theory. [16]

BCS theory describes the transition of superconductors from an ordinary metallic state (*normal state*) to a new state, characterised by vanishing resistivity and perfect diamagnetism. In this *superconducting state* the electronic spectrum develops a gap Δ around the Fermi level, which is maximum at zero temperature and vanishes at the critical temperature T_c . The critical temperature exhibits an *isotope effect*, i.e. T_c increases (or decreases) upon partial replacement of an element with a lighter (heavier) isotope. Isotope effects are also measured for other characteristic properties of superconductors (gap, specific heat, etc.).

BCS theory reconciles all the above experimental observations in a consistent framework, based on three key concepts:

(i) A Fermi sea of electrons in the presence of an attractive interaction is unstable towards the formation of a pair of electrons with opposite spin and momentum (**Cooper pair**), which effectively behaves as a boson. In a superconductor, below T_c , a small, but macroscopic fraction of electrons, of order $\Delta/E_F \simeq 10^{-3}$, forms Cooper pairs – this is sometimes referred to as the *condensate fraction* of a superconductor.

(ii) A variational many-body wavefunction for the electrons is constructed from a superposition of ordinary single-particle states and Cooper pairs (**BCS wavefunction**). The existence of a condensate fraction leads to the appearance of a gap in the electronic spectrum $\epsilon_{\mathbf{k}}$, which satisfies the self-consistent equation:

$$\Delta_{\mathbf{k}} = -\frac{1}{2} \sum_{\mathbf{k}, \mathbf{k}'} \frac{V_{\mathbf{k}, \mathbf{k}'} \Delta_{\mathbf{k}'}}{\sqrt{\epsilon_{\mathbf{k}}^2 + \Delta_{\mathbf{k}}^2}} \cdot \tanh \left(\frac{\sqrt{\epsilon_{\mathbf{k}}^2 + \Delta_{\mathbf{k}}^2}}{2T} \right). \quad (1)$$

(iii) Using a simple model for the electron-electron interaction $V_{\mathbf{k}, \mathbf{k}'}$, the so-called **BCS potential**, which is attractive only if the two electrons with wavevector \mathbf{k}, \mathbf{k}' both lie in a small energy shell ω_D around the Fermi energy E_F , Eq. 1 can be solved analytically, and the gap and T_c are given by:

$$\Delta(T=0) \simeq 2\omega_D \exp \left(-\frac{1}{N(E_F)V} \right), \quad k_b T_c = 1.13\omega_D \exp \left(-\frac{1}{N(E_F)V} \right), \quad (2)$$

The original idea of Bardeen, Cooper and Schrieffer is that the attractive interaction V between electrons is mediated by lattice vibrations (phonons); In this case, ω_D is a representative phonon energy scale, such as the Debye frequency; $N(E_F)$ is the electronic Density of States at the Fermi level.

One of the first successes of BCS theory has been the explanation of the isotope effect on T_c : $\alpha_{T_c} = -\frac{d \ln(T_c)}{d \ln(M)} = 0.5$, where M is the ionic mass, as well as the prediction of several *magic ratios*, satisfied in most elemental superconductors: the most famous is probably the ratio $\frac{2\Delta(0)}{k_b T_c} = 3.53$.

However, BCS theory is valid only at weak coupling ($\lambda = N(E_F)V < 0.2 - 0.3$) and instantaneous interactions; these assumptions are not verified in many conventional superconductors, where the actual values of T_c , isotope effect, magic ratios etc are spectacularly different from the BCS predictions. [54].

A quantitative description of the strong-coupling, retarded regime is given by the many-body ME theory, based on a set of self-consistent coupled diagrammatic equations for the electronic and bosonic propagators. [19, 20, 21, 30]. The bosons that mediate the superconducting pairing can be phonons or other excitations of the crystal, such as plasmons or spin fluctuations. [55] Below the critical temperature, electrons are described by a normal and an *anomalous* electronic propagator, the latter accounting for Cooper pairs. ME equations are then obtained from the Dyson's equations for the normal and anomalous propagators; in their most commonly-used, T -dependent form they can be written as:

$$Z(\mathbf{k}, i\omega_n) = 1 + \frac{\pi T}{\omega_n} \sum_{\mathbf{k}'n'} \frac{\delta(\epsilon_{\mathbf{k}'})}{N(E_F)} \frac{\omega_{n'}}{\sqrt{\omega_{n'}^2 + \Delta^2(\mathbf{k}, i\omega_{n'})}} \lambda(\mathbf{k}, \mathbf{k}', n - n') \quad (3)$$

$$\begin{aligned} Z(\mathbf{k}, i\omega_n) \Delta(\mathbf{k}, i\omega_n) &= \pi T \sum_{\mathbf{k}'n'} \frac{\delta(\epsilon_{\mathbf{k}'})}{N(E_F)} \frac{\Delta(\mathbf{k}', i\omega_{n'})}{\sqrt{\omega_{n'}^2 + \Delta^2(\mathbf{k}, i\omega_{n'})^2}} \times \\ &\times [\lambda(\mathbf{k}, \mathbf{k}', n - n') - \mu(\mathbf{k} - \mathbf{k}')] \end{aligned} \quad (4)$$

where $Z(\mathbf{k}, i\omega_n)$ and $Z(\mathbf{k}, i\omega_n) \Delta(\mathbf{k}, i\omega_n)$ are the self-energy of the normal and anomalous electronic propagators, respectively; $i\omega_n = i(2n\pi T + 1)$ are Matsubara frequencies, \mathbf{k}, \mathbf{k}' are the electronic momenta; the δ function restricts the sum over \mathbf{k}' only to electronic states at the Fermi level. The electrons interact through a retarded attractive interaction $\lambda(\mathbf{k}, \mathbf{k}', n - n')$, and an instantaneous Coulomb repulsion $\mu(\mathbf{k} - \mathbf{k}')$. The interaction $\lambda(\mathbf{k}, \mathbf{k}', n - n')$ is usually expressed in terms of an electron-boson spectral function $\alpha^2 F(\mathbf{k}, \mathbf{k}', \omega)$ as :

$$\lambda(\mathbf{k}, \mathbf{k}', n - n') = \int_0^\infty d\omega \frac{2\omega}{(\omega_n - \omega_{n'})^2 + \omega^2} \alpha^2 F(\mathbf{k}, \mathbf{k}', \omega) \quad (5)$$

Eqs. (3-4) can be solved numerically to obtain the gap, and other thermodynamic quantities. It is very common, and in most cases sufficiently accurate, to approximate the more general form with an isotropic version, replacing the sums on the electronic momenta (\mathbf{k}, \mathbf{k}') with Fermi surface averages. If one is only interested in the T_c , there are excellent approximation formulas; a very popular choice for phonon-mediated superconductors is the Mc-Millan-Allen-Dynes expression: [56]

$$T_c = \frac{\omega_{\text{log}}}{1.2k_B} \exp \left[-\frac{1.04(1 + \lambda)}{\lambda - \mu^*(1 + 0.62\lambda)} \right], \quad (6)$$

where $\lambda = 2 \int d\omega \frac{\alpha^2 F(\omega)}{\omega}$ and $\omega_{\text{log}} = \exp \left[\frac{2}{\lambda} \int \frac{d\omega}{\omega} \alpha^2 F(\omega) \ln(\omega) \right]$ are the ep coupling constant and logarithmic averaged phonon frequency, respectively; μ^* is the so-

called Morel-Anderson pseudopotential, obtained by screening the full Coulomb potential up to a characteristic cut-off energy. [57]

3.2 Ab-initio methods:

The two methods described in this section, *ab-initio* anisotropic Migdal-Eliashberg Theory (DFT-ME in the following) [30, 7] and Superconducting Density Functional Theory (SCDFT), [58, 26, 27] represent a fundamental step forward in the study of actual superconductors, because they permit to obtain a full characterization of the normal and superconducting state of a system from the sole knowledge of the chemical composition and crystal structure. Although there are fundamental and practical differences between the two, both methods rely crucially on the ability of DFT of providing accurate electronic and bosonic spectra for most materials at an affordable computational cost. [59, 52]

The basic assumptions are the following:

1. *Electronic quasi-particles* appearing in Eqs. (3-4) are replaced by the Kohn-Sham quasi-particles.
2. *Bosonic* excitation energies and electron-boson spectral functions are obtained from Density Functional Perturbation Theory (DFPT). [52]

For *phonons*, the spectral function is:

$$\alpha^2 F_{ph}(\mathbf{k}, \mathbf{k}', \omega) = N(E_F) \sum_{\mathbf{v}} g_{\mathbf{k}\mathbf{k}',\mathbf{v}} \delta(\omega - \omega_{\mathbf{k}-\mathbf{k}',\mathbf{v}}), \quad (7)$$

where $g_{\mathbf{k},\mathbf{k}'} = \langle \mathbf{k}' | \delta V_{scf}^{\mathbf{v},\mathbf{k}'-\mathbf{k}} | \mathbf{k} \rangle$ is the *ep* matrix element for the mode \mathbf{v} ; and $\delta V_{scf}^{\mathbf{v},\mathbf{q}}$ is the variation of the Kohn-Sham self-consistent potential due to an infinitesimal displacement along the eigenvector of the phonon mode \mathbf{v} with wave-vector $\mathbf{q} = \mathbf{k}' - \mathbf{k}$.

For *spin fluctuations*, the spectral function is proportional to the imaginary part of the longitudinal interacting spin susceptibility $\chi_{zz}(\mathbf{q} = \mathbf{k} - \mathbf{k}', \omega)$ [60], which, using linear response within the time-dependent-Density-Functional-Theory (TDDFT) framework, [61] can be written as:

$$\chi_{zz}(\mathbf{q}, \omega) = \frac{\chi^{KS}(\mathbf{q}, \omega)}{1 - f_{xc}(\mathbf{q}, \omega) \chi^{ks}(\mathbf{q}, \omega)}, \quad (8)$$

where $\chi^{KS}(\mathbf{q}, \omega)$ is the Kohn-Sham susceptibility, and $f_{xc}(\mathbf{q}, \omega)$ is the exchange and correlation kernel. [62]

3. The *Coulomb potential* $\mu(\mathbf{k} - \mathbf{k}')$ which, in most empirical approaches, is treated as an adjustable parameter within the Morel-Anderson approximation, [57] is treated fully *ab-initio* screening the bare Coulomb potential within RPA. Substantial deviations from typical values of $\mu^* = 0.1 - 0.15$ are found in strongly anisotropic systems such as MgB₂ and layered superconductors; in

some cases, such as alkali metals at high pressure, the effect of Coulomb interactions is even stronger, giving rise to plasmonic effects. [45]

Once the spectra of the quasi-particles and the interactions between them are known from first-principles, DFT-ME or SCDFT can be applied to describe the superconducting state. DFT-ME theory amounts to solving the fully anisotropic ME equations, for electronic and bosonic spectra computed in DFT; The current implementations solve the equations in Matsubara frequencies, and use Padé approximants to continue them to real space. The obvious advantage of this method is that all quantities have an immediate physical interpretation through many-body theory.

SCDFT is a fundamentally different approach, that generalizes the original Hohenberg-Kohn idea of one-to-one correspondence between ground-state density and potential, [63] introducing two additional densities (and potentials) for the ionic system $\Gamma(\mathbf{R}_i)(V_{ext}(\mathbf{R}_i))$ and the superconducting electrons $\chi(\mathbf{r}, \mathbf{r}')(\Delta(\mathbf{r}, \mathbf{r}'))$, and finding the values that minimize a suitable energy functional. This permits to derive a gap equation which is analogous to the BCS one, but instead of an empirical potential contains a *kernel* with all the relevant physical information on the system. I refer the reader to the original references for a full derivation, [26, 27, 58] and to Ref. [6] for an excellent pedagogical introduction.

SCDFT equations are more easily solvable on a computer than fully anisotropic ME equations because they do not require expensive sums over Matsubara frequencies; however, the interpretation of many physical quantities, including the frequency-dependence of the gap, is not equally transparent and straightforward. Another intrinsic limitation is that, like in all DFT-like methods, the quality of the results depends strongly on the quality of the functional.

The latest-developed functionals yield results with an *accuracy* comparable to that of the best DFT-ME calculations, which for most conventional superconductors is between 5 and 10% of the critical temperature. The most severe source of inaccuracy in DFT calculations for superconductors is usually an underconverged integration in reciprocal space in Eqs. (3-4), an issue that has considerably improved thanks to the use of Wannier interpolation techniques.

Achieving quantitative accuracy for conventional pairing also encouraged to address *ab-initio* effects, which are often disregarded even in model approaches, such as anharmonicity, vertex corrections, and zero-point effects. [64, 65, 66]

These turned out to be relevant for a wide variety of compounds, particularly for the newly-discovered superconducting hydrides, where the energy scales of phonons and electrons are comparable. [31, 67, 68] I refer the reader to the relevant references for an in-depth discussion.

For unconventional superconductors, on the other hand, the most severe source of inaccuracy is intrinsic and is the possible divergence in the spin-fluctuation propagator, which completely destroys the predictive power of DFT approaches for currently available functionals. Moreover, most unconventional superconductors suffer from the lack of accuracy of DFT in strongly correlated systems. [69]

3.3 Developments in related fields: *ab-initio* Material Design

The term *ab-initio* Material design indicates the combination of methods for *ab-initio* crystal structure prediction and thermodynamics to predict the behaviour of materials at arbitrary conditions of pressure and temperature, knowing only the initial chemical composition of the system. The development of these methods represents a substantial step forward in computational condensed matter research, as it overcomes one of its biggest limitations, exemplified by the *Maddox Paradox* (1988): ‘*One of the continuing scandals in the physical sciences is that it remains in general impossible to predict the structure of even the simplest crystalline solids from a knowledge of their chemical composition*’.

The basic working principle of *ab-initio* crystal structure prediction is quite simple. Predicting the crystal structure of a material for a given regime of chemical composition and pressure amounts to finding the global minimum of a complicated landscape, generated by the *ab-initio* total energies (or enthalpies) of all possible structures. The number of possible configurations for a typical problem is so large that a purely enumerative approach is unfeasible; in the last years, several methods have been devised to make the problem computationally manageable, such as *ab-initio* random structure search, minima hopping, metadynamics, genetic algorithms, particle swarm algorithms, etc. [47]

Once the most favorable crystal structure for a given composition and pressure is known, the *ab-initio* Calphad (CALculation of PHAse Diagrams) approach permits to predict accurate **phase diagrams**, [70] as illustrated in Fig. 2. The binary Li-S phase diagram in panel (a) shows the stability ranges of different Li-S compositions and has been constructed repeating several *convex hull* calculations at different pressures.

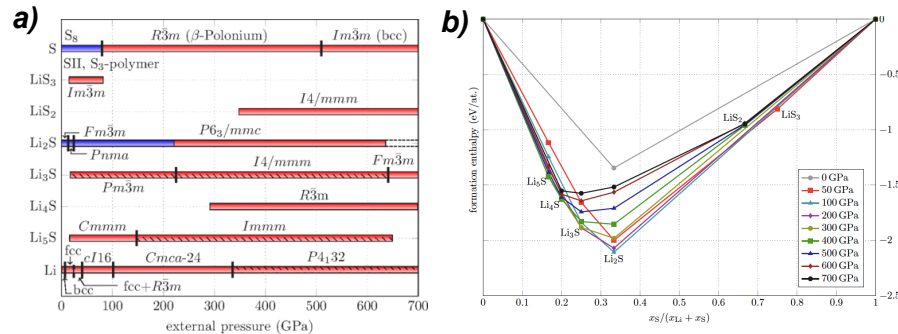


Fig. 2 Basic steps of *ab-initio* materials prediction, readapted from Ref. [71]: the complete phase diagram of a binary alloy as a function of pressure (a) can be constructed combining several convex hull constructions at different pressures (b) (*see text*).

The *convex hull* construction is shown in panel (b). The points represent the lowest-energy structure predicted by an evolutionary search for a given composition; for a binary phase with composition A_xB_y , the formation enthalpy ΔH is defined as: $\Delta H = H(A_xB_y) - [xH(A) + yH(B)]$. If this quantity is negative, the phase A_xB_y is stable with respect to elemental decomposition; if it is positive, the phase is highly (or weakly) metastable, i.e., if formed, it will decompose into its elemental constituents in finite time. However, the decomposition into the two elements is often not the relevant one, as a compound could decompose into other phases, preserving the correct stoichiometry. To estimate all possible decompositions for the binary system, one constructs the most convex curve connecting the formation enthalpy of all known phases for a given stoichiometry. Points on this convex hull represent stable compositions into which phases which lie above the convex hull will decompose into given a sufficient interval of time. The figure also shows that, as pressure increases, the diversity of the phase diagram increases, i.e. off-stoichiometry compositions become possible (*forbidden chemistry*). The convex hull construction can be easily extended to multinary systems (Gibbs diagrams) and finite temperatures including entropic effects.

4 Materials:

The aim of this section is to illustrate how, within a little bit more than a decade, an increased understanding of material-specific aspects of superconductivity gained from *ab-initio* calculations has permitted to replace empirical rules to search for new superconductors with quantitative strategies.

I will start with a general discussion that determine the T_c of conventional superconductors (Sect. 4.1), introducing the concepts of *dormant ep* interactions and lattice instabilities, and showing how these can be used to interpret both the old empirical knowledge (Matthias' rules and Cohen-Anderson limit) and the latest experimental discoveries. [51, 72, 73, 74, 75]

I will then use a toy numerical model (simple graphite), to see how these concepts are realized in an actual physical system, and a very simple approximation to doping (rigid-band) to simulate the effect of physical doping and detect the sources of *ep* interaction in graphite-like materials. Both models are useful for a first exploration, but inadequate to make accurate predictions for actual superconductors, where the doping is usually obtained via chemical substitution, which causes a major rearrangement of phononic and electronic states, and hence sizable changes in the values of the *ep* interaction and T_c .

For simple graphite, nature provides two simple realizations of two of its sources of dormant *ep* interactions: MgB_2 , a prototype of *covalent* superconductors, and graphite intercalated compounds, where superconductivity is correlated with the filling of *interlayer* states. In Sect.4.3 and 4.4 I will discuss these two examples in detail, and also indicate the main theoretical predictions and experimental discoveries which were inspired by them.

In particular, the line of research on covalent superconductors culminated in the discovery of high- T_c conventional superconductivity at extreme pressures in SH_3 , discussed in Sect. 4.5, which also represents a fundamental step forward in the direction of the search of new superconductors using first-principles methods.

After describing the incredible evolution of the state of research in conventional superconductors, in Sect. 4.6 I will present a representative example of unconventional superconductors, iron pnictides and chalcogenides (Fe-based superconductors), discovered in 2008, which shares many similarities with the high- T_c cuprates. This example will allow me to give an idea of the many challenges that theory faces in the description of unconventional superconductors, already in the normal state, and currently represent a fundamental obstacle to the derivation of numerical methods to compute T_c 's.

4.1 Conventional Superconductors: Search Strategies

Matthias' rules The so-called Matthias' rules are a set of empirical rules that summarize the understanding of superconductors in the 70's. The rules were allegedly formulated, and revised several times, by Bernd Matthias, one of the leading material scientists in superconductivity: they are usually cited in this form:

1. High symmetry is good, cubic symmetry is the best.
2. High density of electronic states is good.
3. Stay away from oxygen.
4. Stay away from magnetism.
5. Stay away from insulators.
6. Stay away from theorists.

Matthias' rules were inspired by A15 superconductors (cubic transition metal alloys, which can be easily doped, exhibit sharp peaks in the electronic DOS, and are prone to lattice and magnetic instabilities), and clearly disproved by subsequent experimental discoveries: cuprates and pnictides (first, third, fourth and fifth rule), [3, 4] but also conventional superconductors such as MgB_2 [34] (first and second rule). [1] However, their impact on superconductivity research has been so important that they are still sometimes cited as arguments against conventional superconductivity or the possibility of theoretically predicting new superconductors, together with another old quasi-empirical rule, the Cohen-Anderson limit.

In order to derive more general, non-empirical strategies to search for new superconductors, I will begin with a simple analytical model. Instead the full complexity of the electronic and vibrational properties of real superconductors, for the moment I consider an ideal case, in which a single phonon branch with frequency

ω and a single electronic band with Density of States at the Fermi level $N(E_F)$ are coupled through an average matrix element I . In this case, the T_c is well described by the Mc-Millan-Allen-Dynes formula (Eq. 6) with all constant factors set to one, $\omega_n = \omega$, and the coupling constant is given by the Hopfield expression: $\lambda = (N(E_F)I^2)/(M\omega^2)$:

$$T_c = \frac{\omega}{k_B} \exp \left[-\frac{(1+\lambda)}{\lambda - \mu^*(1+\lambda)} \right], \quad (9)$$

These formulas indicate that there are three main strategies to optimise the critical temperature of a conventional superconductor: (i) maximize the value of the the electronic DOS at the Fermi level $N(E_F)$ (first two Matthias' rules); (ii) select compounds which contain light elements (and stiff bonds), to maximise the characteristic lattice energy scales (ω); and (iii) increase the ep matrix elements (I).

While the first two strategies were already understood in the early 70's, it became apparent only with the MgB_2 discovery that it is possible to find compounds where the intrinsic ep matrix elements I are much larger than in transition metals and their alloys, where the maximum T_c does not exceed 25 K. In a seminal paper, An and Pickett [35] pointed out that the (relatively) high T_c of MgB_2 occurs because of “*covalent bonds driven metallic*”.

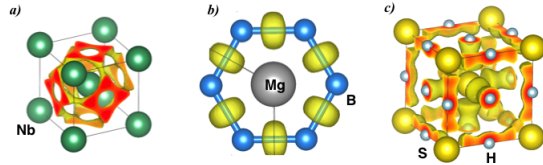


Fig. 3 Electronic localization function in conventional superconductors: bcc Nb ($T_c=9$ K); MgB_2 ($T_c=39$ K); SH_3 ($T_c=203$ K).

The reason why covalent metals have larger intrinsic ep coupling than ordinary metals can be intuitively understood looking at Fig. 3, which shows isosurfaces of the Electronic Localization Function (ELF) for three different superconductors: Nb ($T_c=9\text{K}$), MgB_2 ($T_c=39$ K) and SH_3 ($T_c=203\text{K}$). The ELF indicates regions where electrons are concentrated. It is clear that in MgB_2 and SH_3 , the electrons localize along the bonds, while in Nb they are delocalized over the whole volume. When atoms undergo phonon vibrations, electrons localized along a bond will feel a much stronger perturbation than those spread out over the whole crystal. However, the arguments above are oversimplified, as the existence of strong directional bonds is a necessary prerequisite for large ep coupling, but it is not sufficient: due to the small energy scales involved in the superconducting pairing, it is also essential that the electronic states which contribute to this bond lie at the Fermi level, otherwise they remain *dormant*, and do not contribute to the superconducting pairing. More precisely, this means that shifting the position of the Fermi level (E_F) selects different matrix elements g in Eq. (7) when performing averages over the Fermi surfaces in

in Eqs. (3), (4), and the ep interaction λ , and hence T_c , is appreciable only for some positions of E_F .

A possible strategy to search for new conventional superconductors thus amounts to identifying, first, possible **dormant ep interactions** within a given material class and, second, physical mechanisms to activate them, such as doping, pressure, and alloying. *Ab-initio* approaches permit to explore both steps of this process, at different levels of approximation. In the following I will illustrate the basic working principle, using an example (simple graphite) and two practical realizations (MgB_2 and intercalated graphites); I will also refer to the same principles when discussing possible perspective of future research in Sect. 5.

Before moving on with the discussion, I need to introduce a second concept which is crucial in the search for new conventional superconductors: **lattice instabilities**. This argument is important because it is at the heart of the Cohen-Anderson limit. [22]

According to Eq. (9), T_c can apparently be increased indefinitely, increasing λ , which contradicts what is observed in practice, since the critical temperatures of actual superconductors are limited. However, in my discussion I have so far disregarded the *feedback* effect between phonon frequencies and ep interaction, which is one of the main limiting factors to high- T_c in actual materials. Indeed, the same ep interaction that pairs electrons leading to superconductivity also causes a decrease (softening) of the phonon frequencies. This means that the frequency ω appearing in Mc-Millan's formula for T_c (Eq. 9) should be more correctly rewritten as: $\omega^2 = (\Omega_0)^2(1 - 2\lambda_0)$, where Ω_0 is the bare frequency of the lattice, in the absence of ep interaction, and λ_0 is the corresponding coupling constant. It is now easy to see that the T_c for a fixed Ω_0 has a maximum for a given value of λ_0 and then decreases approaching a lattice instability ($\omega \rightarrow 0$); this means that within a given material class, T_c can only be increased up to a threshold value determined by λ_0 , before incurring in a lattice instability. Using typical parameters for the A15 compounds, which were the best known superconductors when the Cohen-Anderson limit was formulated, gives a maximum value of T_c of ~ 25 K. However, covalent superconductors such as MgB_2 , doped diamond and SH_3 have much larger characteristic phonon scales (Ω_0, λ_0), and can sustain much larger T_c .

4.2 Dormant ep interaction in graphite

To put general arguments on more physical grounds, we now consider a toy model based on an actual physical system, simple graphite, which is realized stacking several layers of graphene on top of each other (the stacking is thus AAA, in contrast to the ABA and ABC stacking of Bernal and rhombohedral graphite); for this experiment, we keep the interlayer distance equal to that of Bernal graphite.

The unit cell contains two inequivalent carbon atoms, that form a hexagonal lattice. This means that the four orbitals of carbon will split into three sp^2 hybrids and a p_z orbital, forming six σ and two π bands, of bonding and anti-bonding char-

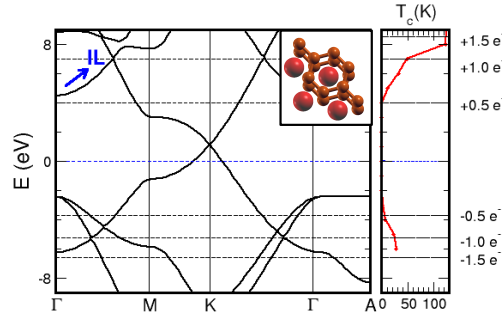


Fig. 4 Rigid-band study of superconductivity in simple graphite; dashed lines indicate the position of the Fermi level for a semi-integer doping of holes or electrons; the blue arrow marks the position of the interlayer band, whose Wannier function is shown in the inset.

acter. The blue arrow points to a fifth band, which has no carbon character: this is the so-called interlayer (IL) band, which is essentially a free-electron state confined between the carbon layers. The relative Wannier function, shown in the inset of the figure, is indeed centered in the middle of the interstitial region between the graphitic layers, and has spherical symmetry. [73, 76]

The phonon spectrum of pure graphite (not shown) is even simpler than its electronic structure: In-plane bond stretching optical phonons form a rather narrow band between 150 and 200 meV, while optical out-of-plane and acoustical modes are more dispersive and extend up to 100 meV.

For the doping of pure graphite, corresponding to four electrons/carbon, the Fermi level cuts the band structure near the crossing point between π and π^* bands, the ep coupling is extremely low, and gives rise to a negligible T_c . However, different *dormant ep* interactions can be activated if, with a *gedankenexperiment*, the Fermi level is shifted to higher or lower energies. This rigid band shift is the simplest approximation to physical doping within an *ab-initio* calculation.

The right panel of Fig. 4 shows a rigid-band calculation of the T_c of simple graphite, in an energy range of ± 8 eV around the Fermi level, corresponding to a doping of ± 1.5 electrons/carbon; in this calculation, the phonons and ep matrix elements are computed only once, for the physical doping of four electrons/carbon, but the averages and sums on the Fermi surface in Eqs. (3-4) are recomputed for different positions of the Fermi level (E_F).

The figure clearly shows that T_c is still negligible for small variations of energy around the original Fermi level, but has a marked increase as soon as holes or electrons are doped into the σ (bonding or antibonding) or IL bands, reaching a maximum of ~ 100 K, when the Fermi level reaches a large van Hove singularity at ~ 8 eV, corresponding to the bottom of the σ^* band. Apart from causing substantial deviations in T_c 's, the coupling of phonons to σ , IL and π electrons is also quali-

tatively different. σ and π electrons couple mostly to high-energy optical phonons, which modulate the interatomic distances in the hexagonal layers, and hence the hopping between neighboring carbon sites; IL electrons, instead, respond to out-of-plane phonons, which modulate their overlap with the π wavefunctions that stick out-of-plane. This effect causes a substantial variation in the shape of the Eliashberg functions (not shown) and ω_{log} . The right scale on Fig. 4 indicates the position of the Fermi level for semi-integer values of hole(-) or electron(+) doping; in both cases, a finite T_c is obtained for a minimum doping of half an electron/carbon is needed, but obtaining a high- T_c requires a much higher doping ($\sim 1 e^-/C$ atom). Note that the highest doping levels that can be obtained with field effect using liquid electrolytes are much lower, i.e. of the order of a few tenths of $e^-/carbon$, so that the only viable alternative to realize superconductivity in doped graphite is via chemical doping.

The rigid-band approximation is instructive to identify dormant ep interactions, but the calculated T_c 's are often severely overestimated compared to other experiments or more sophisticated approximations for doping. In fact, the rigid-band approach neglects important effects due to the self-consistent rearrangement of electrons produced by doping, such as band shifts, renormalization of the phonon frequencies, and screening of the ep matrix elements. [77, 78]

For simple graphite, nature provided two extremely ingenious realizations of our predictions, discussed in the next two sections.

4.3 Magnesium Diboride and other Covalent Superconductors:

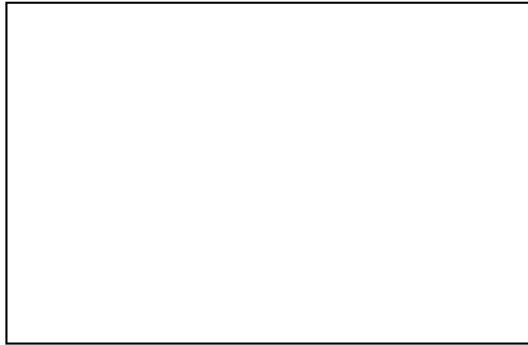


Fig. 5 Two-gap superconductivity in MgB_2 : Anisotropic distribution of the gap on the Fermi surface, predicted by DFT (a) [39]; Evidence of two-gap behaviour from tunneling experiments.(b) [79].

With a T_c of 39 K, magnesium diboride (MgB_2) currently holds the record for conventional superconductivity at ambient pressure. [34, 80] Its crystal structure is layered: boron forms graphite-like hexagonal planes; magnesium is placed in-between, at the center of the hexagons. Mg is completely ionised (Mg^{2+}), and thus MgB_2 is not only isostructural, but also isoelectronic to graphite. However, due to the attractive potential of the Mg ions, the center of mass of the π bands is shifted

up with respect to that of the σ bands compared to simple graphite, so that MgB_2 behaves effectively as a compensated (semi)-metal. The σ holes and π electrons form two cylinders around the center and a 3D tubular network around the corners of the Brillouin zone, respectively, as shown in Fig. 5 (a).

The two group of electronic states experience a rather different coupling to phonons: over 70% of the total ep coupling, in fact, comes from σ holes and bond-stretching phonons; the rest is distributed over the remaining phonon modes and electronic states. [36] The simplest approximation to account for the strong anisotropy of the ep coupling over the Fermi surface is to replace the ep coupling constant λ in Eq. (3-4), with 2×2 matrices of the form: [40]

$$\lambda = \begin{pmatrix} \lambda_{\sigma\sigma} & \lambda_{\sigma\pi} \\ \lambda_{\pi\sigma} & \lambda_{\pi\pi} \end{pmatrix} = \begin{pmatrix} 1.02 & 0.30 \\ 0.15 & 0.45 \end{pmatrix} \quad (10)$$

When the interband coupling is finite but appreciably smaller than the intraband one, $|\lambda_{\sigma\pi} + \lambda_{\pi\sigma}| < |\lambda_{\sigma\sigma} + \lambda_{\pi\pi}|$, the theory predicts that experiments should observe two distinct gaps, closing at the same T_c . [81] Two gap superconductivity was indeed observed by different experimental techniques: specific heat, tunneling, Angle-Resolved Photoemission Spectroscopy (ARPES) for the first time in MgB_2 . [40]

Indeed, in most superconductors, multiband and anisotropic effects are extremely difficult to detect because they are suppressed by the interband scattering induced by sample impurities; in MgB_2 the real-space orthogonality of the σ and π electronic wavefunctions prevents interband scattering, and two-gap superconductivity can be detected also by techniques with a limited resolution. [40]

Fig. 5(b) shows in- and out-of-plane tunneling spectra of MgB_2 , which permit to unambiguously identify a σ (large) and π (small) gap. [79] The experimental spectra compare extremely well with the theoretical prediction of two different gaps on the σ and π sheets of the Fermi surface; the image in the left panel of the figure shows an anisotropic DFT-ME calculation of the gap; in the figure, the color of the Fermi surface is proportional to the size of the gap on that sheet. [39]

Besides providing the first clear case of two-gap superconductivity, MgB_2 is the first example of superconductivity from *doping covalent bonds*. The most spectacular realization of this possibility came in 2004, with the report of a T_c of 4 K in heavily boron-doped diamond, raised to 11 K in thin films. [41, 82]

Diamond is a wide-band insulator ($\Delta \sim 5.5$ eV); when boron is doped at small concentrations, an acceptor band forms within the gap. At the much higher doping levels ($\sim 1 - 10\%$) realized in superconducting samples, the impurity band overlaps so strongly with the valence band of diamond, that the net effect of B doping is to create holes at the top of the valence band. [83] This band is formed by the bonding combination of the four carbon sp^3 hybrids. Boron-doped diamond can thus be seen as a 3D analogue of MgB_2 , where, similarly to MgB_2 , a small fraction of σ holes created by B doping exhibits an extremely strong coupling to bond-stretching phonons.

Since the ep coupling is concentrated in a single type of phonon modes and electronic states, the simplified formulas introduced in Sect. 4.1 give a reasonable

approximation to T_c for both MgB_2 and diamond. [84, 85, 86, 87, 88] Furthermore, they permit to understand why, even though the C-C bonds in diamond are actually stiffer than the B-B bonds in MgB_2 , the measured T_c 's are much lower. In fact, near the bottom (or top) of a band, i.e. at low dopings, the DOS increases as \sqrt{E} in 3D, while it is virtually constant in 2D. This implies that, as holes or electrons are doped into the system, $N(E_F)$, and hence λ , increases much more slowly in 3D systems than in 2D ones. Thus, for physical ranges of dopings the maximum T_c in doped semiconductors is typically very low. [84, 42]

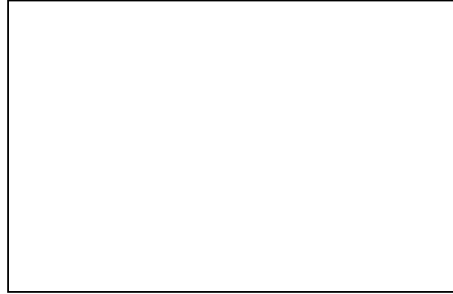


Fig. 6 Electron-phonon coupling (top) and T_c (bottom) as a function of doping in different carbon-based superconductors. Adapted from Ref. [89].

A very ingenious strategy attain high- T_c conventional superconductivity in a doped sp^3 system avoiding negative dimensionality effects was proposed a few years later by Savini et al. [89], i.e. realizing superconductivity in p-doped graphane (fully hydrogenated graphene). Graphane can be considered a 2D version of diamond, in which the bonding is still sp^3 , hence the matrix elements are as large as those of diamond, but the DOS is 2D, hence λ is sizable already at low dopings. For this compound, the authors of Ref. [89] estimate a T_c of ~ 90 K already for 1% doping. Figure 6, from the original reference, compares the behaviour of T_c with doping in the difference class of carbon-based superconductors discussed so far.

Although not as spectacular as graphane, in general many carbon-based compounds doped with boron are good candidates for superconductivity with relatively high temperatures. For example, recent experiments indicate that Q-carbon, an amorphous form of carbon, in-between diamond and graphite, can achieve T_c 's as high as 56 K upon boron doping. [80]

A complementary idea is that of doping boron-rich phases with carbon; boron, being an electron-deficient material, forms a variety of structures with two- and three-center bonds. One of the most common motifs is the icosahedron (B_{12}), found, for example, in the α and β phases of elemental boron, as well as in superconducting dodecaborides. [90] Boron icosahedra doped with carbon are predicted to superconduct with T_c 's as high as 37 K. [91]

4.4 Intercalated Graphites

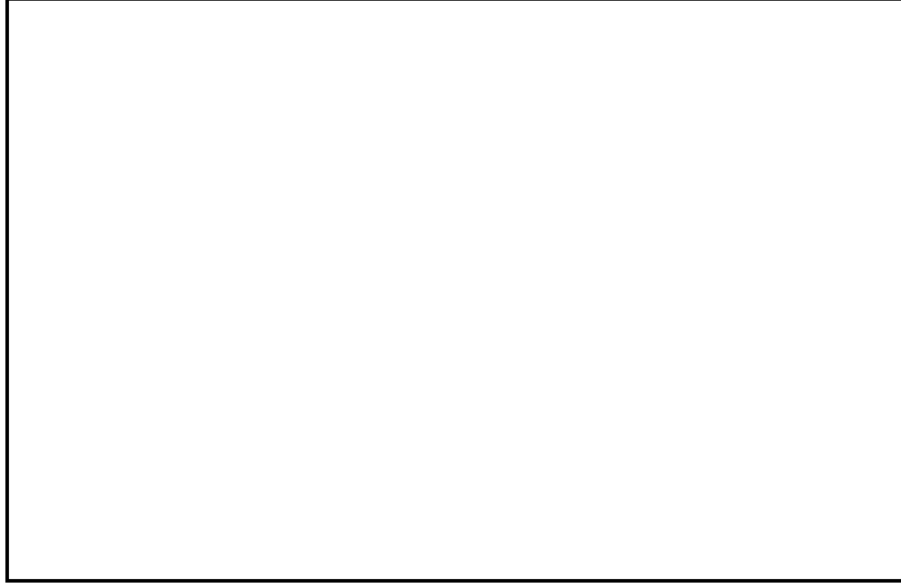


Fig. 7 Physical properties of superconducting graphite intercalation compounds: (a) Dependence of T_c on the interlayer separation in different GICs; [92]; (b) Anisotropic superconducting gap predicted from SCDFT calculations in CaC_6 , [93]; (c) Superconducting gap measured by ARPES in Li-decorated graphene. [94]

While MgB_2 can be considered a natural realization of hole-doped graphite σ bonds, superconducting graphite intercalation compounds (GICs) are the practical realization of superconductivity by doping into the interlayer states. Although the T_c 's are substantially lower than in covalent metals, this type of superconductivity is quite interesting, because it can be more easily manipulated by external means (doping, pressure), and also realized in “artificial” systems, such mono- and bilayers of graphene decorated with alkali or noble metals.

Intercalated graphites had been extensively studied in the 70s, because of their high mobilities, but the only known superconducting member of the family, KC_8 , had an extremely small $T_c (< 1\text{K})$. Only in 2005, superconductivity with relatively high T_c 's was reported in several AC_6 compounds: CaC_6 ($T_c=11.5\text{ K}$), YbC_6 ($T_c=6.5\text{ K}$), and later SrC_6 ($T_c=1.6\text{ K}$). [43, 92] At the same time, it was observed that for all newly-discovered members of the family, the occurrence of superconductivity clearly correlates with the filling of the interlayer band, which is empty in non-superconductors. [76]

A strong correlation is also found between the T_c and the distance between two subsequent graphitic layers in different AC_6 compounds – Fig. 7(a). This can be

easily explained within the conventional ep scenario, [95, 96, 73, 92] since, as demonstrated in Sect. 4.1, when localized due to doping and confinement effects, interlayer electrons can couple to π electrons through out-of-plane phonons of the carbon layers (in GICs, additional coupling is also provided by intercalant modes).

Like in MgB_2 , the distribution of the ep interaction, and hence of the superconducting gap, is very anisotropic on the Fermi surface, being much larger for the interlayer electrons – central sphere in Fig. 7(b) – than for π ones, which form the outer tubular manifold.

The idea superconductivity due to the localization of interlayer states was exploited in Ref. [75], proposing to achieve to superconductivity in Li-decorated graphene. A T_c of 5.9 K, close to the theoretical prediction of 8.6 K, in 2015 in Ref. [94]. Fig. 7(c) shows the superconducting gap, measured by ARPES. Note that also in this case there is a visible variation of the gap between π and IL sheets of the Fermi surface.

4.5 High- T_c Conventional Superconductivity in High Pressure Hydrides

The most spectacular realization of high- T_c conventional superconductivity from doped covalent bonds can be found in SH_3 , which, so far, holds the T_c the record among all (conventional and unconventional) superconductors.

Indeed, superconductivity at high pressures is a rather ubiquitous phenomenon, because high pressures tend to increase the hopping between neighbouring sites and hence metallicity. Almost all the elements of the periodic table can be made superconducting; the typical T_c 's are rather low, reaching a maximum of ~ 20 K in Li, Ca, Sc, Y, V, B, P, S, [97] well reproduced by *ab-initio* calculations. [98, 99, 100, 101]

Hydrogen and its compounds represent a notable exception, having provided, in 2014, the first example of high- T_c conventional superconductivity. This discovery was the coronation of a 50-years long search, inspired by two insightful papers by Neil Ashcroft, predicting high- T_c superconductivity in metallic hydrogen (1968) and covalent hydrides (2004). [102, 103] Both predictions rely on the general arguments for high- T_c conventional superconductivity introduced in section 4.1, i.e. large phonon frequencies due to the light hydrogen mass (*ii*) combined with large ep matrix elements due to the lack of screening from core electrons (*iii*) can yield remarkable superconducting transition temperatures, even if the Density of States at the Fermi level is moderate (*i*).

In 1968, the first of Ashcroft's predictions, superconductivity in metallic hydrogen, seemed merely an academic speculation. The pressure required to metallize hydrogen, which is a large gap insulator at ambient pressure ($\Delta \sim 10$ eV), was clearly beyond reach for the experimental techniques of the time. However, fifty years later, high-pressure research has advanced to such a point that at least three groups have reported evidences of hydrogen metallization, at pressures ranging from 360 to 500 GPa (3.6 to 5 Mbar).[104, 105, 106]

These reports are still controversial, since the pressure ranges are close to the limit of current high-pressure techniques. [107, 108] The insulator-to-metal transition has two possible origins: band overlap, in the molecular *CmCa* phase, or a structural transition to an atomic $\beta - Sn$ phase. The two phases are almost impossible to discern experimentally because hydrogen is a poor X-Ray scatterer, and theoretical studies also predict an unusual spread of values (300-500) GPa for the transition boundary between the two phases, due to the different approximations used to account for quantum lattice effects. [109] However, according to DFT calculations, both the *CmCa* and the $\beta - Sn$ structures should become superconducting at or above ambient temperature, suggesting that the first of Ashcroft's predictions may soon be realized. [110, 111, 112]

The second prediction, superconductivity in covalent hydrides, was experimentally verified at the end of 2014. The underlying idea is that in covalent hydrides, metallization of the hydrogen sublattice should occur at lower pressure than in pure hydrogen, because the other atoms exert an additional chemical pressure.

Indeed, in 2008, superconductivity was measured in compressed silane (SiH_4) at 120 GPa, but the measured T_c (17 K) was disappointingly low compared to theoretical prediction of 100 K. [113, 114] However, this finding proved that the experimental knowledge to make covalent hydrides was available, and it was only a matter of time before high- T_c conventional superconductivity would actually be observed. *Ab-initio* calculations revealed two essential missing pieces of the puzzle: *a*) Megabar pressures can stabilize *superhydrides*, i.e. phases with much larger hydrogen content than the hydrides stable at ambient pressure; *b*) some of these *superhydrides* are metals with unusually strong bonds, which can lead to high- T_c superconductivity. [115]

The first high- T_c superconductor discovered experimentally is a sulfur superhydride (SH_3), which is stabilized under pressure, by compressing gaseous sulfur dihydride (SH_2) in a hydrogen-rich atmosphere. The compound metallizes at ~ 100 GPa, where it exhibits a T_c of 40 K. The T_c increases reaching a maximum of over 203 K at 200 GPa; isotope effect measurements confirmed that superconductivity is of conventional origin. I refer the reader to the original experimental [1, 116, 117, 118] and theoretical [2, 119, 120, 121, 68, 122, 123, 124, 67] references for a more detailed discussion of specific aspects of the SH_3 discovery, such as the nature and thermodynamics of the SH_2 to SH_3 transition, anharmonic and non-adiabatic effects. [125]

In the history of superconducting materials, SH_3 stands out for one main reason: it is the first example of a high- T_c superconductor whose chemical composition, crystal structure and superconducting transition temperature were predicted from first-principles before the actual experimental discovery. In fact, a few months before the experimental report, Duan et al. [2] predicted that SH_2 and H_2 would react under pressure and give rise to a highly symmetric bcc structure, later confirmed by X-Ray experiments, [117] which could reach a T_c as high as 200 K at 200 GPa.

From the point of view of electronic structure, SH_3 is a paradigmatic example of high- T_c conventional superconductivity. Indeed, in this case all three conditions reported in Sect. 4.1 are verified: SH_3 is a hydride, and hence its characteristic vi-

brational frequencies are high (*i*); the Fermi level falls in the vicinity of a van Hove singularity of the DOS of the bcc lattice (*ii*); and the *ep* matrix elements are high due to the unusual H-S covalent bonds stabilized by pressure (*iii*).

Replicating a similar combination is not simple, even in other high-pressure hydrides, where one can hope that high pressure may help stabilize unusual bonding environments and hydrogen-rich stoichiometries. Despite an intense theoretical exploration of the high-pressure superconducting phase diagrams of binary hydrides, [115] only a few candidates match or surpass the T_c of SH_3 : Ca, Y, La. [126, 127]

In fact, the formation of covalent directional bonds between hydrogen and other atoms appears to be very sensitive to their electronegativity difference, [122, 128] and in binary hydrides the possibilities to optimize this parameter are obviously limited. A possible strategy to overcome this limitation is to explore ternary hydrides, where the electronegativity, atomic size, etc. can be tuned continuously combining different elements. However, since ternary Gibb's diagrams are computationally much more expensive than binary convex hulls, fully *ab-initio* studies of ternaries are rare. Two recent studies explore two different strategies towards high- T_c in ternary hydrides: doping low-pressure molecular phases of covalent binary hydrides, like water; [129] and off-stoichiometry phases of alkali-metal alanates and borates, which permit to independently tune the degree of metallicity and covalency. [130]

Due to the intrinsic difficulty of reaching Megabar pressures, and the limited information that can be extracted from X-Ray spectra, the experimental information on high-pressure hydrides is much scarcer than theoretical predictions. Nevertheless, there has been a substantial progress in the last five years: Metallic superhydrides predicted by theory have been reported in hydrides of alkali metals (Li, Na), [131, 132] transition metals (Fe), [133] group-IV elements, etc. For some of these systems, first-principles calculations predict substantial superconducting temperatures, [115] while other cases are controversial. [134, 135, 136]

Resistivity and susceptibility measurements required to detect superconductivity under pressure are even more challenging, and therefore the available information on superconductivity in high-pressure hydrides is still very scarce: besides SH_3 , only one other hydride, PH_3 , has been shown to superconduct at high pressures, albeit with a lower T_c (~ 100 K). [44] At variance with SH_3 , PH_3 is highly metastable, and samples rapidly degrade over time, consistently with *ab-initio* predictions of metastability. [128, 137, 138] SeH_3 , which should exhibit T_c 's comparable to SH_3 , has been successfully synthesized at the end of last year [139], but superconductivity has not been measured yet.

The same arguments that motivated the search for high- T_c conventional superconductivity in high-pressure hydrides can be applied to other compounds that contain light elements, such as Li, B, C etc. Some of these elements form covalent structures with strong directional bonds already at ambient pressure, and high pressures could be used to optimize doping, stoichiometry, etc. However, element-specific factors can unpredictably affect properties relevant in high-pressure superconductivity. For example, elemental phases of alkali metals at high pressure exhibit a characteristic *interstitial charge localization*, due to avoided core overlap. The same effect,

which is extremely detrimental for conventional superconductivity (charge localized in the interstitial regions has an intrinsically low coupling to phonons), also occurs in many of their compounds. This was shown, for example, for the Li-S system, whose behaviour at high pressure is remarkably different from H-S. [71].

4.6 Unconventional Superconductivity in Fe pnictides and chalcogenides

After illustrating the remarkable progress in the research on conventional superconductors, I have chosen to discuss the single largest class of unconventional superconductors, formed by Fe pnictides and chalcogenides (Fe-based superconductors, FeSC). The T_c 's of these compounds, discovered in 2008, go up to 56 K in the bulk, and allegedly up to 100 K in monolayers of FeSe grown on SrTiO₃. [4, 140, 141, 142, 143] Their rich phase diagram, the quasi-2D crystal structure and the unconventional behavior of the superconducting gaps, are strongly reminiscent of the high- T_c cuprates. Thus, I will use FeSC as a representative example to illustrate the challenges faced by *ab-initio* methods in unconventional superconductors, both in the normal and in the superconducting state. [144]

Fig. 8 shows the main features, common to most compounds:

- (a)-(b) A common structural motif, consisting of square planes of iron atoms, and X_4 tetrahedra; X is either a pnictogen (As,P) or a chalcogen (Se,Te).
- (c) A quasi-two-dimensional Fermi surface, comprising two hole and two electron sheets, strongly nested with one other.
- (d) A phase diagram, in which superconductivity sets in after suppressing a spin density wave (SDW) ordered state, by means of doping or pressure. The most common SDW pattern is a stripe one, in which the Fe spins are aligned ferromagnetically along one of the edges of the Fe squares, and antiferromagnetically along the other. The SDW transition is usually preceded by a structural-nematic transition. [145]

FeSC can be grouped in different *families*, depending on the nature of the FeX layers and of the intercalating blocks; the most common are: 11 Fe chalcogenides (FeS, FeSe, FeTe); 111 alkali-metal pnictides (LiFeAs, LiFeP, NaFeAs, NaFeP, etc); 122 pnictides (Ba/KFe₂As₂, BaFe₂P₂, CaFeAs₂, EuFe₂As₂ etc.); 1111 pnictides (LaOFeAs, LaOFeP, etc); 122 chalcogenides (KFe₂Se₂, etc.). In most of these cases, superconductivity appears around a Fe d^6 configuration, but it survives up to high hole or electron dopings in 122 K pnictides and chalcogenides.

In most FeSC, the superconducting gap exhibits a feature which is distinctive of unconventional superconductors, i.e. changes sign over the Fermi surface. According to Eq. 1, this is only possible if, unlike *ep* interaction, the pairing interaction $V_{\mathbf{k},\mathbf{k}'}$ is repulsive over some regions of reciprocal space.

In contrast to the cuprates, where the Fermi surface topology favors *d*-wave superconductivity, the gap of most FeSC exhibits a characteristic s^\pm symmetry, with

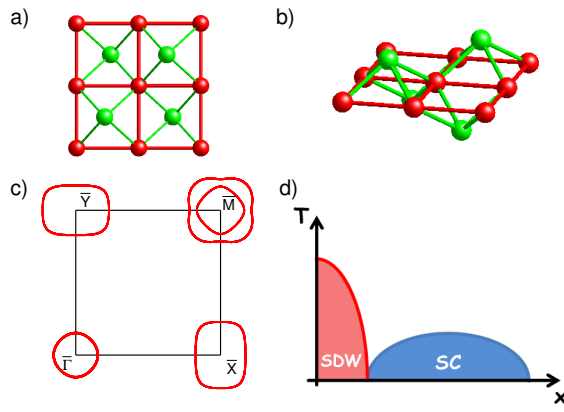


Fig. 8 Common features of Fe-based superconductors (FeSC): FeX layers, seen from the top (a) and side (b); Fe and X atoms are red and green, respectively. (c) Two-dimensional Fermi surface of LaOFeAs, from Ref. [146], with the hole and electron pockets centered at \bar{X} , \bar{Y} and \bar{M} respectively. Here a third hole pocket at $\bar{\Gamma}$ is also present. (d) Phase diagram, showing the transition from SDW to superconducting (SC) state; x is an external tuning parameter (doping, pressure).

opposite signs on the hole and electron sheets of the Fermi surface. However, substantial variations in the symmetry and magnitude of the superconducting gap are observed among and within different FeSC families, which can be related to changes in the general shape and orbital distribution of Fermi surface sheets. [147]

The general topology of the Fermi surface is well described by DFT calculations; however, quasi-particle bands measured by ARPES exhibit renormalizations and shifts, which hint to strong local correlation effects beyond DFT, which require the use of specialized methods, such as DFT+DMFT. [148]

Figure 9 (a), from Ref. [149], shows the Fermi surfaces calculated within DFT (upper panel) and DFT+DMFT (lower panel) for representative FeSC: LaFePO, BaFe₂As₂, LiFeAs, KFe₂As₂. The first three are d^6 pnictides, with the typical hole-electron topology shown in Fig. 8, eventually deformed due to interlayer hopping. [146] In KFe₂As₂, where the electron count is $d^{5.5}$, the hole pocket is expanded and the electron pocket has lost its typical circular shape.

The figure shows that, in most cases, the inclusion of electronic correlation modifies the Fermi surface quantitatively, but not qualitatively, with respect to the DFT prediction. The renormalization of the quasi-particle band dispersion depends on their orbital character, being stronger for Fe t_2 (xz, yz, xy) than for e ($x^2 - y^2, 3z^2 - 1$) orbitals, and on the nature of the X atom; correlation effects are in fact weakest for $X=P$, and increase moving to As, S, Se and Te . [150, 149] Orbital-selective mass renormalizations and poor Fermi liquid behavior are characteristic of a special correlation regime, known as the *Hund's metal* regime, which has been extensively studied by several authors; [151, 152, 153, 149] excellent reviews can be found in Refs. [154, 155].

A very important consequence of the interplay between metallicity, strong correlations, and multiband character in FeSC is their anomalous magnetic behavior. Early DFT studies pointed out that magnetism cannot be consistently described

within neither the itinerant (Slater), nor the localized (Heisenberg) scenario. [156, 157] A regime which is intermediate between the two cannot be treated in DFT, which is a mean-field theory, but requires methods able to capture the *dynamics* of the magnetic moments at different frequency scales. [149, 158, 159, 160, 161, 162].

Panel (c) shows a DFT+DMFT calculation of the magnetically ordered state for a variety of FeSC. [149] Circles (and stars) indicate the theoretical (experimental) value of the ordered SDW magnetic moment, which shows large variations among different compounds. Chalcogenides exhibit large ordered moments, while 111 and 1111 pnictides and phosphides exhibit smaller values. (Grey) squares indicate the value of the local magnetic moment, which oscillates over a much smaller range of values around $2.5 \mu_B$. In the SDW phase the two moments coexist; when the itinerant moment is suppressed with doping or pressure, only the local moment survives, meaning that in the non-magnetic regions of the phase diagram FeSC are in a paramagnetic state.

The superconducting state that emerges from this complicated normal state is clearly unconventional. According to linear response calculations, *ep* coupling plays a marginal role in the superconducting pairing, since the values of the calculated coupling constant λ in all FeSC is extremely small, even including magnetoelastic effects.² [74, 164, 165] The strongest candidate as superconducting mediator are spin fluctuations, as suggested by the unconventional symmetry of the superconducting gap and the proximity of SDW and superconductivity in the phase diagram. [166, 167, 168] As discussed in Sect. 3.2, there is currently no first-principles theory of spin fluctuations with an accuracy comparable to that for *ep* interaction. Most studies of superconductivity in FeSC have therefore adopted a *hybrid* approach, in which the electronic structure in the vicinity of the Fermi level is downfolded or projected to an effective analytical tight-binding model, [169, 170, 171, 146] and electron-electron interactions leading to spin and charge fluctuations are included at a second stage with many-body techniques. The most common are the Random-Phase-Approximation (RPA), Fluctuation Exchange (FLEX), Functional renormalization Group (fRG). [166, 172, 147, 173] Although not quantitatively predictive, these *weak coupling* approaches have provided a detailed understanding of the superconducting gap symmetry, competition of superconductivity with other ordered phases and occurrence of nematic order, and traced their common origin to multi-orbital physics. [174] Fig. 9 (c), from Ref. [170], shows that the variations in T_c across different 1111 pnictides can be reproduced within RPA and derive from changes in orbital composition of the Fermi surface.

A first, very elegant, fully first-principles study of superconductivity in FeSC was carried out by the Gross' group, who applied their recently-derived *ab-initio* theory for spin fluctuations to FeSe – see Sect. 3.2 for details. Fig. 9 (d) shows the superconducting gap calculated in SCDFT, which exhibits an s^\pm symmetry, consistently

² This result is generally accepted, although DFT+DMFT studies evidenced a strong renormalization of some phonon modes, due to strong electronic correlations; [163] *ep* coupling has also been suggested to play a primary role in the enhancement of the superconducting T_c in FeSe monolayers grown on SrTiO₃, [143] although in this case the modes involved in the pairing belong to the substrate.

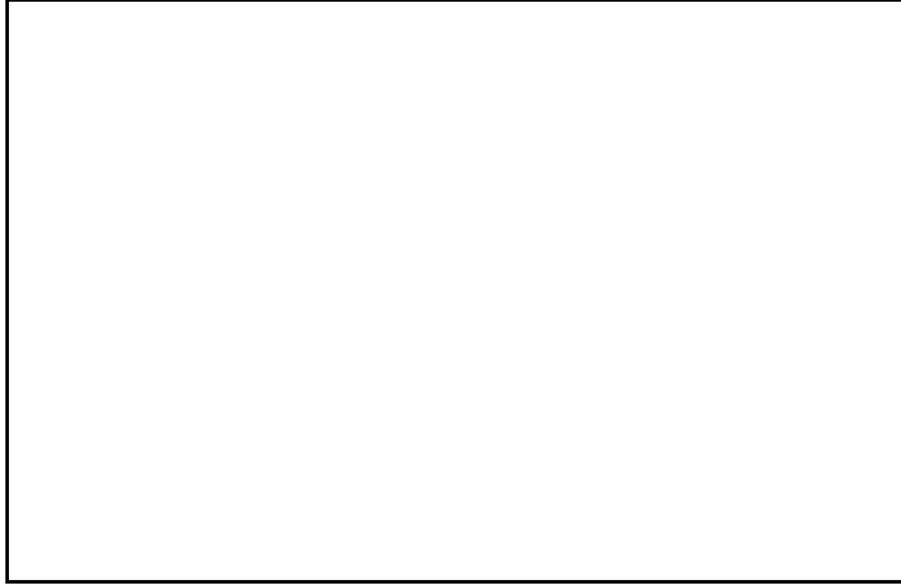


Fig. 9 Normal and superconducting-state properties of FeSC, predicted by DFT+many-body methods. *a*) Renormalization of the Fermi surfaces and *b*) variation of the ordered and local magnetic moment across different families of FeSC, predicted by in DFT+DMFT; [149] *c*) Superconducting trends in 1111 pnictides predicted by DFT+RPA, Ref. [170]; *d*) Superconducting gap of FeSe predicted by SCDFT. [33]

with previous *hybrid* studies. It is important to remark, however, that the gap in Fig. 9 (*d*) was calculated treating the contributions of all pairing channels (phonons, spin fluctuations, charge fluctuations) on equal footing, and without any intermediate mapping on an effective many-body model. However, even this calculation cannot be considered fully *ab-initio* as, in order to obtain a physically meaningful value for the superconducting gap and T_c , the authors had to introduce an artificial *scaling* factor in the spin fluctuation propagator, which would otherwise diverge. [32, 175]

The divergence is associated to the specific choice of TDDFT exchange functional (Adiabatic Local Density Approximation, ALDA) made by the authors which, being the Time-dependent equivalent to the standard local Density Approximation (LDA), overestimates the tendency to magnetism in FeSC. [156] Proposals to cure this critical divergence in a non-empirical fashion are underway, [176] and could lead to a very important step forward in the understanding of unconventional superconductors. However, it is also important to stress that, even if divergence issues are solved, T_c computed within DFT may still be inaccurate, because it neglects renormalization effects of quasi-particle energies and interaction vertices due to strong local electronic correlations, which, in some FeSC, may be sizable. [69, 177]

5 Outlook and Perspectives

The results described in this chapter show that in the last twenty years there has been a substantial advancement in the understanding of superconductors, driven by the progress of *ab-initio* electronic structure methods. The SH₃ discovery has demonstrated that room-temperature superconductivity can be attained, at least at extreme pressures, [1] and that *ab-initio* methods can be very effectively employed to predict new superconductors. The next challenge in the field is clearly to devise practical strategies to replicate the same result at ambient conditions, exploiting novel synthesis and doping techniques. Obviously, the development of *ab-initio* methods that can treat these regimes is a crucial step in this direction.

The aim of this final section is to give a short overview of promising strategies to high-T_c superconductivity, exemplified in Fig. 10 (a)-(e).

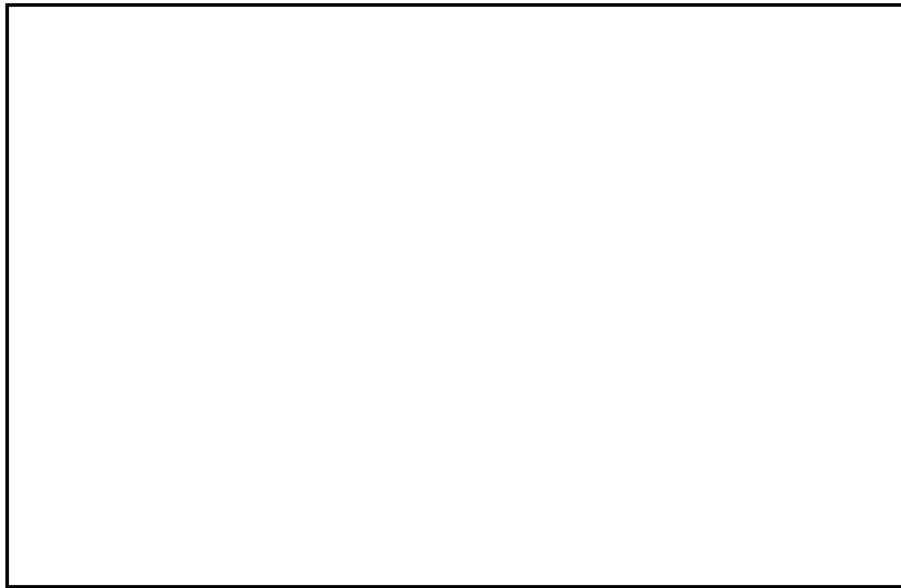


Fig. 10 Selected literature examples of possible strategies to room-temperature superconductivity at ambient pressures: (a) First-principles prediction of α and β -LiB [178] (*Design by Analogy*); (b) Superconductivity in doped ices [129] (*Chemical Doping of molecular crystals*); (c) Charge-density profile of superconducting Pb@Si(111) surface. [179] (*Atomic-scale design and Dimensionality*); (d) High-pressure superconducting phase diagram of phosphorus [101] (*Quenching of High-pressure metastable phases*); (e) T_c vs field effect and chemical doping in monolayer MoS₂ [180] (*Doping by field effect*).

- a) **Design by Analogy:** This is one of the most common routes to search for new superconductors, i.e. achieve high-T_c designing materials with a similar geom-

etry, chemistry, electronic structure, etc. as the best existing superconductors. This route led to several predictions of high- T_c superconductivity in layered borides and carbides after the discovery of MgB_2 , as well as hole-doped LiBC, and, more recently, doped graphane. [181, 182, 89] The main drawback of many of these early works is that the many of these hypothetical compounds are thermodynamically unstable. Nowadays, studies of the thermodynamic stability of compounds are well established, but were very rare at the time of the MgB_2 discovery. One of the first studies to take this aspect into account the prediction of superconductivity in LiB, [178] shown in Fig. 10(a).

- b) **Chemical Doping of Molecular Crystals:** Similarly to covalent solids, molecular ones exhibit stiff bonds, and hence their electronic states can couple strongly to lattice vibrations, which is a prerequisite for high- T_c conventional superconductivity. However, similarly to covalent solids, molecular ones are usually insulating at ambient pressures. Making them superconducting requires either very high pressures, or chemical doping, which is often hard to control experimentally and to model *ab-initio*.

One of the most complete studies of the effect of doping on superconductivity in molecular crystals is the study of superconductivity in doped ice, by Flores-Livas et al. [129] Here, analyzing the effect of different dopants using supercells, the authors found that nitrogen acts as an effective dopant at the oxygen site, leading to a T_c of 60 K. The study nicely evidences the crucial difference between actual doping, modelled with supercells, and more approximate approaches, as rigid-band or jellium doping.

- c) **Atomic-Scale Design and Dimensionality:** Another recent trend in condensed matter research opened by the development of novel techniques, such as Molecular Beam Epitaxy (MBE), or exfoliation, [183] is the design of materials at the atomic scale, through heterostructuring, controlled deposition, strain engineering, etc. This permits to tune superconductivity in existing materials, induce it in semi-conductors and semi-metals through doping, like Li-decorated graphene and phosphorene, or create completely artificial superconductors, depositing superconducting elements on semiconductor surfaces, as in Fig. 10(c), which shows a SCDFT calculation for Pb on the 111 surface. [184, 179] For this type of problems, real-space approaches may be more appropriate than reciprocal space ones. [185]
- d) **Quenching of High-Pressure Metastable Phases** down to ambient pressure is another very attractive route to stabilize unusual bonding environments, enabled by recent developments in high-pressure techniques. In fact, controlled heating and cooling cycles permit to selectively stabilize different metastable phases, realizing pressure-hysteresis cycles. Figure 10 (d), from Ref. [101], shows the crystal structures of the different phases that form the complicated superconducting phase diagram of elemental phosphorus. In this element, a high- T_c branch, clearly distinct from the low- T_c ground-state one, can be accessed by laser heating, and is associated with metastable black phosphorus; similar branchings between high- T_c and low- T_c phases have been predicted at higher pressures.

- e) Doping via **Field Effect** is an attractive route to tune the properties of materials continuously, without impurities and distortions associated to chemical doping. Modern techniques based on liquid electrolytes permit to achieve doping levels as high as $10^{15} \text{ carriers/cm}^3$, corresponding to tenths of electrons, around three orders of magnitude larger than standard solid-state techniques. The first successful applications have been to cuprates, ZrNiCl, and 2D materials –Fig. 10 (e). Rigorous modelling of field-effect devices has been derived in Refs. [186, 187].

Although not an experimental technique, methods for machine learning, which can be used to pre-screen *ab-initio* proposals, will most likely play a bigger and bigger role in the design and discovery of new materials. [188]

Note that all of the specific examples discussed above are based on the assumption of *conventional* (phonon-mediated) pairing. The same techniques have been, and can be, applied also to *unconventional* superconductors, which remain the likeliest candidates for high- T_c superconductivity. However, without a quantitative theory of the superconducting pairing, it is at the moment impossible to formulate reliable predictions of T_c and other superconducting properties. A progress in this direction is therefore an essential prerequisite to any meaningful computational search.

Acknowledgements There are many people who, over the years, helped me to shape my view on superconductivity. Many of these encounters turned into friendships, and I am very grateful for that. A special thank goes to my mentors in Rome (Luciano Pietronero, Giovanni Bachelet) and Stuttgart (Jens Kortus and Ole Krogh Andersen), who introduced me to the field of superconductivity and electronic structure, as well as to all my collaborators and students, with whom I had the pleasure to work and argue on many topics. Thanks to José Flores-Livas, Christoph Heil, Renato Gonnelli, Bernhard Keimer, Jun Sung Kim, Rheinhard Kremer, Igor Mazin, Paolo Postorino, Gianni Profeta and Antonio Sanna for the many discussions and projects we shared over the years.

I would never have completed this chapter without the help of my current office neighbor, Paolo Dore, who enquired about the status of the project almost every day, and of Luca de’ Medici, Christoph Heil, Antonio Sanna and Alessandro Toschi, who gave me suggestion on parts of the manuscript at different stages. Finally, I would like to dedicate this work to the memory of two very special people, Sandro Massidda and Ove Jepsen, that I will always remember for their kindness, culture, and enthusiasm for physics. I miss them both.

References

1. A. P. Drozdov, M. I. Erements, I. A. Troyan, V. Ksenofontov, and S. I. Shylin, “Conventional superconductivity at 203 kelvin at high pressures in the sulfur hydride system,” *Nature*, vol. 000, p. 2015/08/17/online, 2015.
2. D. Duan, Y. Liu, F. Tian, D. Li, X. Huang, Z. Zhao, H. Yu, B. Liu, W. Tian, and T. Cui, “Pressure-induced metallization of dense (h2s)2h2 with high-tc superconductivity,” *Sci. Rep.*, vol. 4, p. 6968, Nov 2014.
3. J. Bednorz and K. Mueller *Zeit. Phys. B*, vol. 64, p. 189, 1986.
4. Y. Kamihara, T. Watanabe, M. Hirano, and H. Hosono, “Iron-based layered superconductor LaOFeAs,” *Journal of the American Chemical Society*, vol. 130, no. 11, p. 32963297, 2008.
5. F. Giustino, “Electron-phonon interactions from first principles,” *Rev. Mod. Phys.*, vol. 89, p. 015003, Feb 2017.

6. A. Sanna, "Introduction to superconducting density functional theory," [url=https://www.cond-mat.de/events/correl17/manuscripts/sanna.pdf](https://www.cond-mat.de/events/correl17/manuscripts/sanna.pdf), 2017.
7. A. Sanna, J. A. Flores-Livas, A. Davydov, G. Profeta, K. Dewhurst, S. Sharma, and E. K. U. Gross, "Ab initio eliashberg theory: Making genuine predictions of superconducting features," *Journal of the Physical Society of Japan*, vol. 87, no. 4, p. 041012, 2018.
8. M. Sato and Y. Ando, "Topological superconductors: a review," *Reports on Progress in Physics*, vol. 80, no. 7, p. 076501, 2017.
9. R. A. Klemm, "Pristine and intercalated transition metal dichalcogenide superconductors," *Physica C: Superconductivity and its Applications*, vol. 514, pp. 86 – 94, 2015. Superconducting Materials: Conventional, Unconventional and Undetermined.
10. H. Boschker and J. Mannhart, "Quantum-matter heterostructures," *Annual Review of Condensed Matter Physics*, vol. 8, no. 1, pp. 145–164, 2017.
11. C. Chu, L. Deng, and B. Lv, "Hole-doped cuprate high temperature superconductors," *Physica C: Superconductivity and its Applications*, vol. 514, pp. 290 – 313, 2015. Superconducting Materials: Conventional, Unconventional and Undetermined.
12. O. Gunnarsson, "Superconductivity in fullerides," *Rev. Mod. Phys.*, vol. 69, pp. 575–606, Apr 1997.
13. Y. Kasahara, K. Kuroki, S. Yamanaka, and Y. Taguchi, "Unconventional superconductivity in electron-doped layered metal nitride halides $m\text{N}_x$ ($m=\text{Ti, Zr, Hf}$; $x=\text{Cl, Br, I}$)," *Physica C: Superconductivity and its Applications*, vol. 514, pp. 354 – 367, 2015. Superconducting Materials: Conventional, Unconventional and Undetermined.
14. H. K. Onnes *Comm. Phys. Lab. Univ. Leiden*, vol. 133, p. 37, 1913.
15. W. Meissner and R. Ochsenfeld *Naturwissenschaften*, vol. 21, p. 787, 1933.
16. J. Bardeen, L. N. Cooper, and J. R. Schrieffer, "Theory of superconductivity," *Phys. Rev.*, vol. 108, p. 1175, 1957.
17. A. Migdal, "Migdal's theorem," *Sov. Phys. JETP*, vol. 34, p. 996, 1958.
18. G. M. Eliashberg *Sov. Phys. JETP*, vol. 11, p. 696, 1960.
19. P. Allen and B. Mitrovic, "Theory of superconducting t_c ," *Solid State Physics* **37**, p 1-92, Academic New York, 1982.
20. D. Scalapino, in "Superconductivity", Dekker, New York, pp.1-92 (1969).
21. J. P. Carbotte, "Properties of boson-exchange superconductors," *Rev. Mod. Phys.*, vol. 62, pp. 1027–1157, Oct 1990.
22. M. Cohen and P. Anderson, *Superconductivity in d- and f- band Metals*. American Inst. of Physics, 1972.
23. M. K. Wu, J. R. Ashburn, C. J. Torng, P. H. Hor, R. L. Meng, L. Gao, Z. J. Huang, Y. Q. Wang, and C. W. Chu, "Superconductivity at 93 k in a new mixed-phase y-ba-cu-o compound system at ambient pressure," *Phys. Rev. Lett.*, vol. 58, pp. 908–910, Mar 1987.
24. A. Schilling, M. Cantoni, J. D. Guo, and H. R. Ott, "Superconductivity above 130 k in the hg-ba-ca-cu-o system," *Nature*, vol. 363, p. 56 EP, May 1993.
25. A. Gurevich, "To use or not to use cool superconductors?," *Nature Materials*, vol. 10, p. 255, Mar 2011.
26. M. Lüders, M. A. L. Marques, N. N. Lathiotakis, A. Floris, G. Profeta, L. Fast, A. Continenza, S. Massidda, and E. K. U. Gross, "Ab initio," *Phys. Rev. B*, vol. 72, p. 024545, Jul 2005.
27. M. A. L. Marques, M. Lüders, N. N. Lathiotakis, G. Profeta, A. Floris, L. Fast, A. Continenza, E. K. U. Gross, and S. Massidda, "Ab initio," *Phys. Rev. B*, vol. 72, p. 024546, Jul 2005.
28. F. Giustino, M. L. Cohen, and S. G. Louie, "Electron-phonon interaction using wannier functions," *Phys. Rev. B*, vol. 76, p. 165108, Oct 2007.
29. M. Calandra, G. Profeta, and F. Mauri, "Adiabatic and nonadiabatic phonon dispersion in a wannier function approach," *Phys. Rev. B*, vol. 82, p. 165111, Oct 2010.
30. E. R. Margine and F. Giustino, "Anisotropic migdal-eliashberg theory using wannier functions," *Phys. Rev. B*, vol. 87, p. 024505, Jan 2013.

31. I. Errea, M. Calandra, and F. Mauri, "Anharmonic free energies and phonon dispersions from the stochastic self-consistent harmonic approximation: Application to platinum and palladium hydrides," *Phys. Rev. B*, vol. 89, p. 064302, Feb 2014.
32. F. Essenberg, A. Sanna, A. Linscheid, F. Tanczyk, G. Profeta, P. Cudazzo, and E. K. U. Gross, "Superconducting pairing mediated by spin fluctuations from first principles," *Phys. Rev. B*, vol. 90, p. 214504, Dec 2014.
33. F. Essenberg, A. Sanna, P. Buczek, A. Ernst, L. Sandratskii, and E. K. U. Gross, "Ab initio theory of iron-based superconductors," *Phys. Rev. B*, vol. 94, p. 014503, Jul 2016.
34. J. Nagamatsu, N. Nakagawa, T. Muranaka, Y. Zenitani, and J. Akimitsu, "Superconductivity at 39 K in magnesium diboride," *Nature (London)*, vol. 410, p. 63, 2001.
35. J. M. An and W. E. Pickett, "Superconductivity of MgB_2 : Covalent bonds driven metallic," *Phys. Rev. Lett.*, vol. 86, no. 19, pp. 4366–4369, 2001.
36. Y. Kong, O. V. Dolgov, O. Jepsen, and O. K. Andersen, "Electron-phonon interaction in the normal and superconducting states of MgB_2 ," *Phys. Rev. B*, vol. 64, no. 2, p. 020501, 2001.
37. J. Kortus, I. I. Mazin, K. D. Belashchenko, V. P. Antropov, and L. L. Boyer, "Superconductivity of metallic boron in mgb_2 ," *Phys. Rev. Lett.*, vol. 86, pp. 4656–4659, May 2001.
38. A. Y. Liu, I. I. Mazin, and J. Kortus, "Beyond eliashberg superconductivity in mgb_2 : Anharmonicity, two-phonon scattering, and multiple gaps," *Phys. Rev. Lett.*, vol. 87, p. 087005, Aug 2001.
39. Choi Hyoung Joon, Roundy David, Sun Hong, Cohen Marvin L., and Louie Steven G., "The origin of the anomalous superconducting properties of MgB_2 ," *Nature*, vol. 418, p. 758, aug 2002.
40. I. I. Mazin, O. K. Andersen, O. Jepsen, O. V. Dolgov, J. Kortus, A. A. Golubov, A. B. Kuz'menko, and D. van der Marel, "Superconductivity in mgb_2 : Clean or dirty?," *Phys. Rev. Lett.*, vol. 89, p. 107002, Aug 2002.
41. E. A. Ekimov, V. A. Sidorov, E. D. Bauer, N. Mel'nik, N. J. Curro, J. Thompson, and S. Stishov, "Superconductivity in diamond," *Nature*, vol. 428, p. 542, 2004.
42. Bustarret E., Marcenat C., Achatz P., Kačmarčík J., Lévy F., Huxley A., Ortéga L., Bourgeois E., Blase X., Débarre D., and Boulmer J., "Superconductivity in doped cubic silicon," *Nature*, vol. 444, p. 465, nov 2006.
43. Weller Thomas E., Ellerby Mark, Saxena Siddharth S., Smith Robert P., and Skipper Neal T., "Superconductivity in the intercalated graphite compounds C_6Yb and C_6Ca ," *Nature Physics*, vol. 1, p. 39, sep 2005.
44. A. Drozdov, M. I. Eremets, and I. A. Troyan, "Superconductivity above 100 K in PH_3 at high pressures," *arXiv/cond-mat/1508.06224*, 2015.
45. R. Akashi and R. Arita, "Development of density-functional theory for a plasmon-assisted superconducting state: Application to lithium under high pressures," *Phys. Rev. Lett.*, vol. 111, p. 057006, Aug 2013.
46. C. Grimaldi, L. Pietronero, and S. Straessler, "Nonadiabatic superconductivity: electron-phonon interaction beyond migdal's theorem," *Phys. Rev. Lett.*, vol. 75, p. 1158, 1995.
47. W. S. M. and C. Richard, "Crystal structure prediction from first principles," *Nature Materials*, vol. 7, pp. 937–946, dec 2008.
48. L. Zhang, Y. Wang, J. Lv, and Y. Ma, "Materials discovery at high pressures," *Nature Reviews Materials*, vol. 2, pp. 17005 EP –, Feb 2017. Review Article.
49. G. D. Gaspari and B. L. Gyorffy, "Electron-phonon interactions, d resonances, and superconductivity in transition metals," *Phys. Rev. Lett.*, vol. 28, pp. 801–805, Mar 1972.
50. K. J. Chang, M. M. Dacorogna, M. L. Cohen, J. M. Mignot, G. Chouteau, and G. Martinez, "Superconductivity in high-pressure metallic phases of si," *Phys. Rev. Lett.*, vol. 54, pp. 2375–2378, May 1985.
51. S. Y. Savrasov and D. Y. Savrasov, "Electron-phonon interactions and related physical properties of metals from linear-response theory," *Phys. Rev. B*, vol. 54, p. 16487, 1996.
52. S. Baroni, S. de Gironcoli, A. D. Corso, and P. Giannozzi, "Phonons and related crystal properties from density-functional perturbation theory," *Rev. Mod. Phys.*, vol. 73, p. 515, 2001.

53. N. Marzari, A. A. Mostofi, J. R. Yates, I. Souza, and D. Vanderbilt, "Maximally localized wannier functions: Theory and applications," *Rev. Mod. Phys.*, vol. 84, pp. 1419–1475, Oct 2012.
54. F. Marsiglio and J. P. Carbotte, "Strong-coupling corrections to bardeen-cooper-schrieffer ratios," *Phys. Rev. B*, vol. 33, pp. 6141–6146, May 1986.
55. N. F. Berk and J. R. Schrieffer, "Effect of ferromagnetic spin correlations on superconductivity," *Phys. Rev. Lett.*, vol. 17, pp. 433–435, Aug 1966.
56. P. Allen and R. Dynes, "Transition temperature of strong-coupled superconductors reanalyzed," *Phys. Rev. B*, vol. 12, p. 905, 1975.
57. P. Morel and P. W. Anderson, "Calculation of the superconducting state parameters with retarded electron-phonon interaction," *Phys. Rev.*, vol. 125, pp. 1263–1271, Feb 1962.
58. L. N. Oliveira, E. K. U. Gross, and W. Kohn, "Density-functional theory for superconductors," *Phys. Rev. Lett.*, vol. 60, pp. 2430–2433, Jun 1988.
59. R. O. Jones and O. Gunnarsson, "The density functional formalism, its applications and prospects," *Rev. Mod. Phys.*, vol. 61, pp. 689–746, Jul 1989.
60. G. Vignale and K. S. Singwi, "Effective two-body interaction in coulomb fermi liquids," *Phys. Rev. B*, vol. 32, pp. 2156–2166, Aug 1985.
61. E. Runge and E. K. U. Gross, "Density-functional theory for time-dependent systems," *Phys. Rev. Lett.*, vol. 52, pp. 997–1000, Mar 1984.
62. F. Essenberger, P. Buczek, A. Ernst, L. Sandratskii, and E. K. U. Gross, "Paramagnons in fese close to a magnetic quantum phase transition: Ab initio study," *Phys. Rev. B*, vol. 86, p. 060412, Aug 2012.
63. P. Hohenberg and W. Kohn, "Inhomogeneous electron gas," *Phys. Rev.*, vol. 136, p. B864, 1964.
64. L. Pietronero, S. Straessler, and C. Grimaldi, "Nonadiabatic superconductivity i. vertex corrections for the electron-phonon interactions," *Phys. Rev. B*, vol. 52, p. 10516, 1995.
65. L. Boeri, E. Cappelluti, and L. Pietronero, "Small fermi energy, zero-point fluctuations, and nonadiabaticity in MgB_2 ," *Phys. Rev. B*, vol. 71, p. 012501, Jan 2005.
66. M. Lazzeri, M. Calandra, and F. Mauri, "Anharmonic phonon frequency shift in MgB_2 ," *Phys. Rev. B*, vol. 68, p. 220509, Dec 2003.
67. W. Sano, T. Koretsune, T. Tadano, R. Akashi, and R. Arita, "Effect of van hove singularities on high- T_c superconductivity in H_3S ," *Phys. Rev. B*, vol. 93, p. 094525, Mar 2016.
68. I. Errea and M. Calandra and C. J. Pickard and J. R. Nelson and R. J. Needs and Y. Li and H. Liu and Y. Zhang and Y. Ma and F. Mauri, "Quantum hydrogen-bond symmetrization in the superconducting hydrogen sulfide system," *Nature*, vol. 532, pp. 81–84, 2016.
69. Z. P. Yin, A. Kutepov, and G. Kotliar, "Correlation-enhanced electron-phonon coupling: Applications of gw and screened hybrid functional to bismuthates, chloronitrides, and other high- T_c superconductors," *Phys. Rev. X*, vol. 3, p. 021011, May 2013.
70. H. Lukas, S. G. Fries, and B. Sundman, *Computational Thermodynamics: the Calphad Method*. Cambridge University Press, 2007.
71. C. Kokail, C. Heil, and L. Boeri, "Search for high- T_c conventional superconductivity at megabar pressures in the lithium-sulfur system," *Phys. Rev. B*, vol. 94, p. 060502, Aug 2016.
72. L. Boeri, G. Bachelet, E. Cappelluti, and L. Pietronero, "Small fermi energy and phonon anharmonicity in MgB_2 and related compounds," *Phys. Rev. B*, vol. 65, p. 214501, May 2002.
73. L. Boeri, G. B. Bachelet, M. Giantomassi, and O. K. Andersen, "Electron-phonon interaction in graphite intercalation compounds," *Phys. Rev. B*, vol. 76, p. 064510, Aug 2007.
74. L. Boeri, O. V. Dolgov, and A. A. Golubov, "Is $LaFeAsO_{1-x}F_x$ an electron-phonon superconductor?," *Phys. Rev. Lett.*, vol. 101, p. 026403, Jul 2008.
75. G. Profeta, M. Calandra, and F. Mauri, "Phonon-mediated superconductivity in graphene by lithium deposition," *Nature Phys.*, vol. 8, pp. 131–134, 2012.
76. Csányi Gábor, Littlewood P. B., Nevidomsky Andriy H., Pickard Chris J., and Simons B. D., "The role of the interlayer state in the electronic structure of superconducting graphite intercalated compounds," *Nature Physics*, vol. 1, p. 42, sep 2005.
77. A. Subedi and L. Boeri, "Vibrational spectrum and electron-phonon coupling of doped solid picene from first principles," *Phys. Rev. B*, vol. 84, p. 020508, Jul 2011.

78. M. Casula, M. Calandra, and F. Mauri, "Local and nonlocal electron-phonon couplings in k_3 picene and the effect of metallic screening," *Phys. Rev. B*, vol. 86, p. 075445, Aug 2012.
79. R. S. Gonnelli, D. Daghero, G. A. Ummarino, V. A. Stepanov, J. Jun, S. M. Kazakov, and J. Karpinski, "Direct evidence for two-band superconductivity in MgB_2 single crystals from directional point-contact spectroscopy in magnetic fields," *Phys. Rev. Lett.*, vol. 89, p. 247004, Nov 2002.
80. A. Bhaumik, R. Sachan, and J. Narayan, "High-temperature superconductivity in boron-doped q-carbon," *ACS Nano*, vol. 11, no. 6, pp. 5351–5357, 2017. PMID: 28448115.
81. H. Suhl, B. T. Matthias, and L. R. Walker, "Bardeen-cooper-schrieffer theory of superconductivity in the case of overlapping bands," *Phys. Rev. Lett.*, vol. 3, pp. 552–554, Dec 1959.
82. Y. Takano, M. Nagao, I. Sakaguchi, M. Tachiki, T. Hatano, K. Kobayashi, H. Umezawa, and H. Kawarada, "Superconductivity in diamond thin films well above liquid helium temperature," *Applied Physics Letters*, vol. 85, no. 14, pp. 2851–2853, 2004.
83. T. Yokoya, T. Nakamura, T. Matsushita, T. Muro, Y. Takano, M. Nagao, T. Takenouchi, H. Kawarada, and T. Oguchi, "Origin of the metallic properties of heavily boron-doped superconducting diamond," *Nature*, vol. 438, pp. 647 EP –, Dec 2005.
84. L. Boeri, J. Kortus, and O. K. Andersen, "Three-dimensional MgB_2 -type superconductivity in hole-doped diamond," *Phys. Rev. Lett.*, vol. 93, p. 237002, Nov 2004.
85. K.-W. Lee and W. E. Pickett, "Superconductivity in boron-doped diamond," *Phys. Rev. Lett.*, vol. 93, p. 237003, Nov 2004.
86. X. Blase, C. Adessi, and D. Connétable, "Role of the dopant in the superconductivity of diamond," *Phys. Rev. Lett.*, vol. 93, p. 237004, Nov 2004.
87. F. Giustino, J. R. Yates, I. Souza, M. L. Cohen, and S. G. Louie, "Electron-phonon interaction via electronic and lattice wannier functions: Superconductivity in boron-doped diamond reexamined," *Phys. Rev. Lett.*, vol. 98, p. 047005, Jan 2007.
88. M. Hoesch, T. Fukuda, J. Mizuki, T. Takenouchi, H. Kawarada, J. P. Sutter, S. Tsutsui, A. Q. R. Baron, M. Nagao, and Y. Takano, "Phonon softening in superconducting diamond," *Phys. Rev. B*, vol. 75, p. 140508, Apr 2007.
89. G. Savini, A. C. Ferrari, and F. Giustino, "First-principles prediction of doped graphane as a high-temperature electron-phonon superconductor," *Phys. Rev. Lett.*, vol. 105, p. 037002, Jul 2010.
90. B. T. Matthias, T. H. Geballe, K. Andres, E. Corenzwit, G. W. Hull, and J. P. Maita, "Superconductivity and antiferromagnetism in boron-rich lattices," *Science*, vol. 159, no. 3814, pp. 530–530, 1968.
91. M. Calandra, N. Vast, and F. Mauri, "Superconductivity from doping boron icosahedra," *Phys. Rev. B*, vol. 69, p. 224505, Jun 2004.
92. J. S. Kim, L. Boeri, J. R. O'Brien, F. S. Razavi, and R. K. Kremer, "Superconductivity in heavy alkaline-earth intercalated graphites," *Phys. Rev. Lett.*, vol. 99, p. 027001, Jul 2007.
93. A. Sanna, G. Profeta, A. Floris, A. Marini, E. K. U. Gross, and S. Massidda, "Anisotropic gap of superconducting CaC_6 : A first-principles density functional calculation," *Phys. Rev. B*, vol. 75, p. 020511, Jan 2007.
94. B. M. Ludbrook, G. Levy, P. Nigge, M. Zonno, M. Schneider, D. J. Dvorak, C. N. Veenstra, S. Zhdanovich, D. Wong, P. Dosanjh, C. Straßer, A. Stöhr, S. Forti, C. R. Ast, U. Starke, and A. Damascelli, "Evidence for superconductivity in Li-decorated monolayer graphene," *Proceedings of the National Academy of Sciences*, vol. 112, no. 38, pp. 11795–11799, 2015.
95. M. Calandra and F. Mauri, "Theoretical explanation of superconductivity in CaC_6 ," *Phys. Rev. Lett.*, vol. 95, p. 237002, Nov 2005.
96. J. S. Kim, L. Boeri, R. K. Kremer, and F. S. Razavi, "Effect of pressure on superconducting Ca-intercalated graphite CaC_6 ," *Phys. Rev. B*, vol. 74, p. 214513, Dec 2006.
97. J. Hamlin, "Superconductivity in the metallic elements at high pressures," *Physica C: Superconductivity and its Applications*, vol. 514, pp. 59 – 76, 2015. Superconducting Materials: Conventional, Unconventional and Undetermined.
98. G. Profeta, C. Franchini, N. N. Lathiotakis, A. Floris, A. Sanna, M. A. L. Marques, M. Lüders, S. Massidda, E. K. U. Gross, and A. Continenza, "Superconductivity in lithium,

- potassium, and aluminum under extreme pressure: A first-principles study,” *Phys. Rev. Lett.*, vol. 96, p. 047003, Feb 2006.
99. Y. Yao, D. D. Klug, J. Sun, and R. Martoňák, “Structural prediction and phase transformation mechanisms in calcium at high pressure,” *Phys. Rev. Lett.*, vol. 103, p. 055503, Jul 2009.
 100. M. Monni, F. Bernardini, A. Sanna, G. Profeta, and S. Massidda, “Origin of the critical temperature discontinuity in superconducting sulfur under high pressure,” *Phys. Rev. B*, vol. 95, p. 064516, Feb 2017.
 101. J. A. Flores-Livas, A. Sanna, A. P. Drozdov, L. Boeri, G. Profeta, M. Eremets, and S. Goedecker, “Interplay between structure and superconductivity: Metastable phases of phosphorus under pressure,” *Phys. Rev. Materials*, vol. 1, p. 024802, Jul 2017.
 102. N. Ashcroft, “Metallic hydrogen: A high-temperature superconductor?,” *Phys. Rev. Lett.*, vol. 21, pp. 1748–1749, Dec 1968.
 103. N. Ashcroft, “Hydrogen dominant metallic alloys: High temperature superconductors?,” *Phys. Rev. Lett.*, vol. 92, p. 187002, May 2004.
 104. E. G. Dalladay-Simpson, R. T. Howie, “Evidence for a new phase of dense hydrogen above 325 gigapascals,” *Nature*, vol. 529, pp. 63–67, 2016.
 105. M. Eremets, I. Troyan, and A. Drozdov, “Low temperature phase diagram of hydrogen at pressures up to 380 GPa. A possible metallic phase at 360 GPa and 200 K,” *arXiv/cond-mat/1601.04479*.
 106. R. P. Dias and I. F. Silvera, “Observation of the wigner-huntington transition to metallic hydrogen,” *Science*, vol. 355, no. 6326, pp. 715–718, 2017.
 107. M. Eremets and A. P. Drozdov, “Comments on the claimed observation of the wigner-huntington transition to metallic hydrogen,” *arxiv-condmat/1702.05125*, 2017.
 108. A. F. Goncharov and V. V. Struzhkin, “Comment on observation of the wigner-huntington transition to metallic hydrogen,” *arXiv preprint arXiv:1702.04246*, 2017.
 109. J. M. McMahon, M. A. Morales, C. Pierleoni, and D. M. Ceperley, “The properties of hydrogen and helium under extreme conditions,” *Rev. Mod. Phys.*, vol. 84, pp. 1607–1653, Nov 2012.
 110. P. Cudazzo, G. Profeta, A. Sanna, A. Floris, A. Continenza, S. Massidda, and E. K. U. Gross, “Ab initio description of high-temperature superconductivity in dense molecular hydrogen,” *Phys. Rev. Lett.*, vol. 100, p. 257001, Jun 2008.
 111. J. M. McMahon and D. M. Ceperley, “High-temperature superconductivity in atomic metallic hydrogen,” *Phys. Rev. B*, vol. 84, p. 144515, Oct 2011.
 112. M. Borinaga, I. Errea, M. Calandra, F. Mauri, and A. Bergara, “Anharmonic effects in atomic hydrogen: Superconductivity and lattice dynamical stability,” *Phys. Rev. B*, vol. 93, p. 174308, May 2016.
 113. M. I. Eremets, I. A. Trojan, S. A. Medvedev, J. S. Tse, and Y. Yao, “Superconductivity in hydrogen dominant materials: Silane,” *Science*, vol. 319, no. 5869, pp. 1506–1509, 2008.
 114. Y. Li, G. Gao, Y. Xie, Y. Ma, T. Cui, and G. Zou, “Superconductivity at ~100 k in dense $\text{SiH}_4(\text{H}_2)_2$ predicted by first principles,” *Proceedings of the National Academy of Sciences*, vol. 107, no. 36, pp. 15708–15711, 2010.
 115. E. Zurek, R. Hoffmann, N. Ashcroft, A. R. Oganov, and A. O. Lyakhov, “A little bit of lithium does a lot for hydrogen,” *Proc. Natl. Acad. Sci. U.S.A.*, vol. 106, no. 42, pp. 17640–17643, 2009.
 116. A. F. Goncharov, S. S. Lobanov, I. Kruglov, X.-M. Zhao, X.-J. Chen, A. R. Oganov, Z. Konôpková, and V. B. Prakapenka, “Hydrogen sulfide at high pressure: Change in stoichiometry,” *Phys. Rev. B*, vol. 93, p. 174105, May 2016.
 117. M. Einaga, M. Sakata, T. Ishikawa, K. Shimizu, M. I. Eremets, A. P. Drozdov, I. A. Troyan, N. Hirao, and Y. Ohishi, “Crystal structure of the superconducting phase of sulfur hydride,” *Nature Physics*, vol. 12, pp. 835 EP –, May 2016.
 118. F. Capitani, B. Langerome, J.-B. Brubach, P. Roy, A. Drozdov, M. I. Eremets, E. J. Nicol, J. P. Carbotte, and T. Timusk, “Spectroscopic evidence of a new energy scale for superconductivity in H_3S ,” *Nature Physics*, vol. 13, pp. 859 EP –, Jun 2017. Article.
 119. C. Heil and L. Boeri, “Influence of bonding on superconductivity in high-pressure hydrides,” *Phys. Rev. B*, vol. 92, p. 060508, Aug 2015.

120. Flores-Livas, José, Sanna, Antonio, and Gross, E. K.U., "High temperature superconductivity in sulfur and selenium hydrides at high pressure," *Eur. Phys. J. B*, vol. 89, no. 3, p. 63, 2016.
121. I. Errea, M. Calandra, C. J. Pickard, J. Nelson, R. J. Needs, Y. Li, H. Liu, Y. Zhang, Y. Ma, and F. Mauri, "High-pressure hydrogen sulfide from first principles: A strongly anharmonic phonon-mediated superconductor," *Phys. Rev. Lett.*, vol. 114, p. 157004, Apr 2015.
122. N. Bernstein, C. S. Hellberg, M. D. Johannes, I. I. Mazin, and M. J. Mehl, "What superconducts in sulfur hydrides under pressure and why," *Phys. Rev. B*, vol. 91, p. 060511, Feb 2015.
123. Y. Quan and W. E. Pickett, "Van hove singularities and spectral smearing in high-temperature superconducting h_3S ," *Phys. Rev. B*, vol. 93, p. 104526, Mar 2016.
124. R. Akashi, W. Sano, R. Arita, and S. Tsuneyuki, "Possible "magnéli" phases and self-alloying in the superconducting sulfur hydride," *Phys. Rev. Lett.*, vol. 117, p. 075503, Aug 2016.
125. L. P. Gor'kov and V. Z. Kresin, "Colloquium: High pressure and road to room temperature superconductivity," *Rev. Mod. Phys.*, vol. 90, p. 011001, Jan 2018.
126. H. Wang, J. S. Tse, K. Tanaka, T. Iitaka, and Y. Ma, "Superconductive sodalite-like clathrate calcium hydride at high pressures," *Proc. Natl. Acad. Sci. U.S.A.*, vol. 109, no. 17, pp. 6463–6466, 2012.
127. H. Liu, I. I. Naumov, R. Hoffmann, N. W. Ashcroft, and R. J. Hemley, "Potential high- T_c superconducting lanthanum and yttrium hydrides at high pressure," *Proc. Natl. Acad. Sci. U.S.A.*, vol. 114, no. 27, pp. 6990–6995, 2017.
128. Y. Fu, X. Du, L. Zhang, F. Peng, M. Zhang, C. J. Pickard, R. J. Needs, D. J. Singh, W. Zheng, and Y. Ma, "High-pressure phase stability and superconductivity of pnictogen hydrides and chemical trends for compressed hydrides," *Chem. Mater.*, vol. 28, no. 6, pp. 1746–1755, 2016.
129. J. A. Flores-Livas, A. Sanna, A. Davydov, S. Goedecker, and M. A. L. Marques, "Emergence of superconductivity in doped h_2O ice at high pressure," *arxiv-condmat/1610.04110*.
130. C. Kokail, W. von der Linden, and L. Boeri, "Prediction of high- T_c conventional superconductivity in the ternary lithium borohydride system," *Phys. Rev. Materials*, vol. 1, p. 074803, Dec 2017.
131. C. Pépin, P. Loubeyre, F. Occelli, and P. Dumas, "Synthesis of lithium polyhydrides above 130 gpa at 300 k," *Proceedings of the National Academy of Sciences*, vol. 112, no. 25, pp. 7673–7676, 2015.
132. V. V. Struzhkin, D. Y. Kim, E. Stavrou, T. Muramatsu, H.-k. Mao, C. J. Pickard, R. J. Needs, V. B. Prakapenka, and A. F. Goncharov, "Synthesis of sodium polyhydrides at high pressures," *Nature Communications*, vol. 7, pp. 12267 EP –, Jul 2016. Article.
133. C. M. Pépin, G. Geneste, A. Dewaele, M. Mezouar, and P. Loubeyre, "Synthesis of feh5: A layered structure with atomic hydrogen slabs," *Science*, vol. 357, no. 6349, pp. 382–385, 2017.
134. A. Majumdar, J. S. Tse, M. Wu, and Y. Yao, "Superconductivity in feh₅," *Phys. Rev. B*, vol. 96, p. 201107, Nov 2017.
135. A. G. Kvashnin, I. A. Kruglov, D. V. Semenok, and A. R. Oganov, "Iron superhydrides feh₅ and feh₆: Stability, electronic properties, and superconductivity," *J. Phys. Chem. C*, vol. 122, no. 8, pp. 4731–4736, 2018.
136. L. B. Christoph Heil, Giovanni B. Bachelet, "No superconductivity in iron polyhydrides at high pressures," *arXiv preprint, arXiv:1804.03572*, Apr 2018.
137. J. A. Flores-Livas, M. Amsler, C. Heil, A. Sanna, L. Boeri, G. Profeta, C. Wolverton, S. Goedecker, and E. K. U. Gross, "Superconductivity in metastable phases of phosphorus-hydride compounds under high pressure," *Phys. Rev. B*, vol. 93, p. 020508, Jan 2016.
138. A. Shamp, T. Terpstra, T. Bi, Z. Falls, P. Avery, and E. Zurek, "Decomposition products of phosphine under pressure: Ph₂ stable and superconducting?," *J. Am. Chem. Soc.*, vol. 138, no. 6, pp. 1884–1892, 2016. PMID: 26777416.
139. E. J. Pace, J. Binns, M. P. Alvarez, P. Dalladay-Simpson, E. Gregoryanz, and R. T. Howie, "Synthesis and stability of hydrogen selenide compounds at high pressure," *The Journal of Chemical Physics*, vol. 147, no. 18, p. 184303, 2017.

140. J.-F. Ge, Z.-L. Liu, C. Liu, C.-L. Gao, D. Qian, Q.-K. Xue, Y. Liu, and J.-F. Jia, "Superconductivity above 100 K in single-layer FeSe films on doped SrTiO₃," *Nature Materials*, vol. 14, pp. 285 EP –, Nov 2014.
141. J. Paglione and R. L. Greene, "High-temperature superconductivity in iron-based materials," *Nature Physics*, vol. 6, pp. 645 EP –, Aug 2010. Review Article.
142. D. C. Johnston, "The puzzle of high temperature superconductivity in layered iron pnictides and chalcogenides," *Advances in Physics*, vol. 59, no. 6, pp. 803–1061, 2010.
143. D. Huang and J. E. Hoffman, "Monolayer FeSe on SrTiO₃," *Annual Review of Condensed Matter Physics*, vol. 8, no. 1, pp. 311–336, 2017.
144. D. N. Basov and A. V. Chubukov, "Manifesto for a higher T_c," *Nature Physics*, vol. 7, pp. 272 EP –, Apr 2011. Perspective.
145. R. M. Fernandes, A. V. Chubukov, and J. Schmalian, "What drives nematic order in iron-based superconductors?," *Nature Physics*, vol. 10, pp. 97 EP –, Jan 2014. Review Article.
146. O. Andersen and L. Boeri, "On the multi-orbital band structure and itinerant magnetism of iron-based superconductors," *Annalen der Physik*, vol. 523, no. 1-2, pp. 8–50, 2011.
147. P. J. Hirschfeld, M. M. Korshunov, and I. I. Mazin, "Gap symmetry and structure of Fe-based superconductors," *Reports on Progress in Physics*, vol. 74, no. 12, p. 124508, 2011.
148. G. Kotliar, S. Y. Savrasov, K. Haule, V. S. Oudovenko, O. Parcollet, and C. A. Marianetti, "Electronic structure calculations with dynamical mean-field theory," *Rev. Mod. Phys.*, vol. 78, pp. 865–951, Aug 2006.
149. Yin Z. P., Haule K., and Kotliar G., "Kinetic frustration and the nature of the magnetic and paramagnetic states in iron pnictides and iron chalcogenides," *Nature Materials*, vol. 10, p. 932, Sep 2011.
150. L. de' Medici, G. Giovannetti, and M. Capone, "Selective Mott physics as a key to iron superconductors," *Phys. Rev. Lett.*, vol. 112, p. 177001, Apr 2014.
151. P. Werner, E. Gull, M. Troyer, and A. J. Millis, "Spin freezing transition and non-Fermi-liquid self-energy in a three-orbital model," *Phys. Rev. Lett.*, vol. 101, p. 166405, Oct 2008.
152. K. Haule and G. Kotliar, "Coherence-incoherence crossover in the normal state of iron oxypnictides and importance of Hund's rule coupling," *New Journal of Physics*, vol. 11, no. 2, p. 025021, 2009.
153. L. de' Medici, J. Mravlje, and A. Georges, "Janus-faced influence of Hund's rule coupling in strongly correlated materials," *Phys. Rev. Lett.*, vol. 107, p. 256401, Dec 2011.
154. A. Georges, L. de' Medici, and J. Mravlje, "Strong correlations from Hund's coupling," *Annual Review of Condensed Matter Physics*, vol. 4, no. 1, pp. 137–178, 2013.
155. L. de' Medici, "Hund's metals, explained," *arXiv/cond-mat/1707.03282*.
156. I. I. Mazin, M. D. Johannes, L. Boeri, K. Koepernik, and D. J. Singh, "Problems with reconciling density functional theory calculations with experiment in ferropnictides," *Phys. Rev. B*, vol. 78, p. 085104, Aug 2008.
157. I. I. Mazin and M. D. Johannes, "A key role for unusual spin dynamics in ferropnictides," *Nature Physics*, vol. 5, pp. 141 EP –, Dec 2008. Article.
158. M. Aichhorn, L. Pourovskii, and A. Georges, "Importance of electronic correlations for structural and magnetic properties of the iron pnictide superconductor LaFeAsO," *Phys. Rev. B*, vol. 84, p. 054529, Aug 2011.
159. P. Hansmann, R. Arita, A. Toschi, S. Sakai, G. Sangiovanni, and K. Held, "Dichotomy between large local and small ordered magnetic moments in iron-based superconductors," *Phys. Rev. Lett.*, vol. 104, p. 197002, May 2010.
160. A. Toschi, R. Arita, P. Hansmann, G. Sangiovanni, and K. Held, "Quantum dynamical screening of the local magnetic moment in Fe-based superconductors," *Phys. Rev. B*, vol. 86, p. 064411, Aug 2012.
161. S. L. Skornyakov, A. A. Katanin, and V. I. Anisimov, "Linear-temperature dependence of static magnetic susceptibility in LaFeAsO from dynamical mean-field theory," *Phys. Rev. Lett.*, vol. 106, p. 047007, Jan 2011.
162. T. Schickling, F. Gebhard, J. Bünemann, L. Boeri, O. K. Andersen, and W. Weber, "Gutzwiller theory of band magnetism in LaFeAsO," *Phys. Rev. Lett.*, vol. 108, p. 036406, Jan 2012.

163. S. Mandal, R. E. Cohen, and K. Haule, "Strong pressure-dependent electron-phonon coupling in fese," *Phys. Rev. B*, vol. 89, p. 220502, Jun 2014.
164. L. Boeri, M. Calandra, I. I. Mazin, O. V. Dolgov, and F. Mauri, "Effects of magnetism and doping on the electron-phonon coupling in bafe_2as_2 ," *Phys. Rev. B*, vol. 82, p. 020506, Jul 2010.
165. A. Subedi, L. Zhang, D. J. Singh, and M. H. Du, "Density functional study of fes, fese, and fete: Electronic structure, magnetism, phonons, and superconductivity," *Phys. Rev. B*, vol. 78, p. 134514, Oct 2008.
166. A. V. Chubukov, D. V. Efremov, and I. Eremin, "Magnetism, superconductivity, and pairing symmetry in iron-based superconductors," *Phys. Rev. B*, vol. 78, p. 134512, Oct 2008.
167. K. Kuroki, S. Onari, R. Arita, H. Usui, Y. Tanaka, H. Kontani, and H. Aoki, "Unconventional pairing originating from the disconnected fermi surfaces of superconducting $\text{lafeaso}_{1-x}\text{fx}$," *Phys. Rev. Lett.*, vol. 101, p. 087004, Aug 2008.
168. I. I. Mazin, D. J. Singh, M. D. Johannes, and M. H. Du, "Unconventional superconductivity with a sign reversal in the order parameter of $\text{lafeaso}_{1-x}\text{fx}$," *Phys. Rev. Lett.*, vol. 101, p. 057003, Jul 2008.
169. S. Graser, T. A. Maier, P. J. Hirschfeld, and D. J. Scalapino, "Near-degeneracy of several pairing channels in multiorbital models for the fe pnictides," *New Journal of Physics*, vol. 11, no. 2, p. 025016, 2009.
170. K. Kuroki, H. Usui, S. Onari, R. Arita, and H. Aoki, "Pnictogen height as a possible switch between high- T_c nodeless and low- T_c nodal pairings in the iron-based superconductors," *Phys. Rev. B*, vol. 79, p. 224511, Jun 2009.
171. T. Miyake, K. Nakamura, R. Arita, and M. Imada, "Comparison of ab initio low-energy models for lafepo , lafeaso , bafe_2as_2 , lifecas , fese , and fete : Electron correlation and covalency," *Journal of the Physical Society of Japan*, vol. 79, no. 4, p. 044705, 2010.
172. R. Thomale, C. Platt, J. Hu, C. Honerkamp, and B. A. Bernevig, "Functional renormalization-group study of the doping dependence of pairing symmetry in the iron pnictide superconductors," *Phys. Rev. B*, vol. 80, p. 180505, Nov 2009.
173. C. Platt, R. Thomale, C. Honerkamp, S.-C. Zhang, and W. Hanke, "Mechanism for a pairing state with time-reversal symmetry breaking in iron-based superconductors," *Phys. Rev. B*, vol. 85, p. 180502, May 2012.
174. M. Yi, Y. Zhang, Z.-X. Shen, and D. Lu, "Role of the orbital degree of freedom in iron-based superconductors," *npj Quantum Materials*, vol. 2, no. 1, p. 57, 2017.
175. L. Ortenzi, I. I. Mazin, P. Blaha, and L. Boeri, "Accounting for spin fluctuations beyond local spin density approximation in the density functional theory," *Phys. Rev. B*, vol. 86, p. 064437, Aug 2012.
176. S. Sharma, E. K. U. Gross, A. Sanna, and J. K. Dewhurst, "Source-free exchange-correlation magnetic fields in density functional theory," *Journal of Chemical Theory and Computation*, vol. 14, no. 3, pp. 1247–1253, 2018. PMID: 29420031.
177. L. de' Medici, "Hund's induced fermi-liquid instabilities and enhanced quasiparticle interactions," *Phys. Rev. Lett.*, vol. 118, p. 167003, Apr 2017.
178. A. N. Kolmogorov and S. Curtarolo, "Prediction of different crystal structure phases in metal borides: A lithium monoboride analog to Mgb_2 ," *Phys. Rev. B*, vol. 73, p. 180501, May 2006.
179. A. Linschied, A. Sanna, and E. K. U. Gross, "Ab-initio calculation of a pb single layer on a si substrate: two-dimensionality and superconductivity," *arXiv cond-mat/1503.00977*, 2015.
180. J. T. Ye, Y. J. Zhang, R. Akashi, M. S. Bahramy, R. Arita, and Y. Iwasa, "Superconducting dome in a gate-tuned band insulator," *Science*, vol. 338, no. 6111, pp. 1193–1196, 2012.
181. G. Satta, G. Profeta, F. Bernardini, A. Continenza, and S. Massidda, "Electronic and structural properties of superconducting mgb_2 , casi_2 , and related compounds," *Phys. Rev. B*, vol. 64, p. 104507, Aug 2001.
182. H. Rosner, A. Kitaigorodsky, and W. E. Pickett, "Prediction of high T_c superconductivity in hole-doped libc ," *Phys. Rev. Lett.*, vol. 88, p. 127001, Mar 2002.
183. K. S. Novoselov, A. K. Geim, S. V. Morozov, D. Jiang, Y. Zhang, S. V. Dubonos, I. V. Grigorieva, and A. A. Firsov, "Electric field effect in atomically thin carbon films," *Science*, vol. 306, no. 5696, pp. 666–669, 2004.

184. T. Zhang, P. Cheng, W.-J. Li, Y.-J. Sun, G. Wang, X.-G. Zhu, K. He, L. Wang, X. Ma, X. Chen, Y. Wang, Y. Liu, H.-Q. Lin, J.-F. Jia, and Q.-K. Xue, "Superconductivity in one-atomic-layer metal films grown on si(111)," *Nature Physics*, vol. 6, pp. 104 EP –, Jan 2010.
185. A. Linscheid, A. Sanna, A. Floris, and E. K. U. Gross, "First-principles calculation of the real-space order parameter and condensation energy density in phonon-mediated superconductors," *Phys. Rev. Lett.*, vol. 115, p. 097002, Aug 2015.
186. T. Sohier, M. Calandra, and F. Mauri, "Density-functional calculation of static screening in two-dimensional materials: The long-wavelength dielectric function of graphene," *Phys. Rev. B*, vol. 91, p. 165428, Apr 2015.
187. T. Sohier, M. Calandra, and F. Mauri, "Density functional perturbation theory for gated two-dimensional heterostructures: Theoretical developments and application to flexural phonons in graphene," *Phys. Rev. B*, vol. 96, p. 075448, Aug 2017.
188. S. Curtarolo, G. L. W. Hart, M. Buongiorno Nardelli, N. Mingo, S. Sanvito, and O. Levy, "The high-throughput highway to computational materials design," *Nature Materials*, vol. 12, pp. 191–201, mar 2013.